

12-2021

## **IMMOBILIZED LIPASE ON ZIF FOR ENHANCED BIOFUEL PRODUCTION**

Reem Mohammed Al Mansouri

Follow this and additional works at: [https://scholarworks.uaeu.ac.ae/all\\_theses](https://scholarworks.uaeu.ac.ae/all_theses)

 Part of the [Chemical Engineering Commons](#)

---

United Arab Emirates University

College of Engineering

Department of Chemical and Petroleum Engineering

IMMOBILIZED LIPASE ON ZIF FOR ENHANCED BIOFUEL  
PRODUCTION

Reem Mohammed Al Mansouri

This thesis is submitted in partial fulfilment of the requirements for the degree of  
Master of Science in Chemical Engineering

Under the Supervision of Professor Sulaiman Al Zuhair

December 2021

### Declaration of Original Work

I, Reem Mohammed Al Mansouri, the undersigned, a graduate student at the United Arab Emirates University (UAEU), and the author of this thesis entitled “*Immobilized Lipase on ZIF for Enhanced Biofuel Production*”, hereby, solemnly declare that this thesis is my own original research work that has been done and prepared by me under the supervision of Professor Sulaiman Al Zuhair, in the College of Engineering at UAEU. This work has not previously formed the basis for the award of any academic degree, diploma or a similar title at this or any other university. Any materials borrowed from other sources (whether published or unpublished) and relied upon or included in my thesis have been properly cited and acknowledged in accordance with appropriate academic conventions. I further declare that there is no potential conflict of interest with respect to the research, data collection, authorship, presentation and/or publication of this thesis.

Student's Signature: *R. Almansoori*

Date: 27/12/2021

Copyright © 2021 Reem Mohammed Al Mansouri  
All Rights Reserved

## Approval of the Master Thesis

- 1) Advisor (Committee Chair): Sulaiman Al-Zuhair

Title: Professor

Department of Chemical and Petroleum Engineering

College of Engineering

Signature 

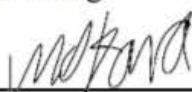
Date 20.01.2022

- 2) Member: Mohamednoor Altarawneh

Title: Associate Professor

Department of Chemical and Petroleum Engineering

College of Engineering

Signature 


Date 20/1/2022

- 3) Member (External Examiner): Vijay Singh

Title: Founder Professor

Department of Agricultural and Biological Engineering

Institution: University of Illinois at Urbana-Champaign, USA

Signature 

Date 20/1/2022

Mohammednoor Altarawneh on behalf of the external examiner

This Master Thesis is accepted by:

Dean of the College of Engineering Professor James Klausner

Signature James F. Klausner Date 14/12/2021

Dean of the College of Graduate Studies: Professor Ali Al-Marzouqi

Signature Ali Hassan Date 22/02/2022

Copy \_\_\_ of \_\_\_

## Abstract

Enzymatic transesterification of triglycerides to produce biodiesel has been gaining increasing attention owing to its advantages over chemical processes. Being catalysts, enzymes are not consumed during the processes in which they are used, and therefore, a successful technique to allow their repeated use can significantly enhance the economic feasibility of the process. The most common approach to allow easy separation of the enzymes and to eliminate their wastage is immobilization on a support matrix. Recently, Metal Organic Frameworks (MOFs) have been suggested as a preferable support for enzyme immobilization, owing to their high-order structure and high porosity and specific surface area.

This thesis presents a study on the use of lipase encapsulated inside hexagonal ZIF-8 for enhance biodiesel production. It was shown that the lipase encapsulation did not have a significant effect on the morphology, surface properties and crystallinity of the ZIF-8 crystals. The effects of methanol ratio, temperature, oil concentration and water content, on the biodiesel production yield and rate of reaction, were tested. The highest yield was obtained at a methanol ratio and temperature of 6:1 and 40°C, respectively. It was also shown that the yield decreased with the increase in water content. The activity and stability of the immobilized lipase in ZIF-8 by encapsulation was compared to that immobilized by surface adsorption. Although the adsorbed lipase on ZIF-8 showed higher activity. At methanol ratio of 12:1, the encapsulated lipase in ZIF-8 maintained 83% residual activity after 5 cycles, compared to only 34% attained by the adsorbed lipase at the same conditions. The experimental results were used to determine the kinetics parameters of modified Ping Pong Bi Bi model, and the accuracy of the prediction were compared to those

obtained by the Michaelis Menten model. To gain a better insight into how the reaction occurs inside the ZIF-8 crystal with encapsulated lipase, a diffusion-reaction model was developed and numerically solved. The results clearly show that the substrate did not diffuse deeply into the crystal, which further confirmed the mass transfer limitation that resulted in the lower activity of the encapsulated lipase as compared to the adsorbed one.

**Keywords:** Biodiesel, Zeolite Imidazolate Framework, Lipase, Finite Difference, Reaction-Diffusion Mode.



## Title and Abstract (in Arabic)

### تجميد الليباز باستخدام ال ZIF لتحسين إنتاج الديزل الحيوي

#### الملخص

اكتسبت عملية تحويل الانزيم لإنتاج وقود الديزل الحيوي اهتماماً متزايداً؛ وذلك لقابلية تطبيقها على مجموعة واسعة من الزيوت الخام دون الحاجة إلى معالجة مسبقة. بالإضافة إلى ذلك، يستخدم الانزيم كحفاز في العملية وبالتالي لا يتم استهلاك الإنزيمات أثناء استخدامها فتصنف هذه الطريقة كواحدة من أنجح الطرق لإعادة استخدام الإنزيم مما يساعد في خفض قيمة التكلفة للعملية، حيث ان الانزيم مكلف. ولمنع الإنزيم من التحلل و فقط نشاطه وتلوثه، تم إقتراح استخدام MOF كمادة داعمة لتثبيت الانزيم. وذلك نظرا لهيكلها الفريد و مساميتها العالية.

تدور هذه الأطروحة حول دراسة استخدام (MOFs) لمادة داعمة للإنزيم لتعزيز إنتاج وقود الديزل الحيوي. حيث تم تغليف الإنزيم بنجاح في أطر زيوليت إيميدازولات سداسية الأضلاع (ZIF-8). وتبين أن تغليف الليباز لم يكن له تأثير في تغيير هيكل وخصائص (ZIF-8). وقد تم دراسة تأثير نسبة تركيز الميثانول وزيت الزيتون، درجة الحرارة المحيط وغيرها وذلك من أجل الحصول على الظروف المثالية لإنتاج وقود الديزل الحيوي. وقد كانت اعلى نسبة زيت الزيتون: للميثانول ودرجة الحرارة المثالية هي 61: و 40°C.

وقد تم التحقق من صحة وفاعلية هذه الآلية من خلال مقارنة استقرار الإنزيم المغلف بتلك التي تم تجميدها بواسطة الامتصاص السطح. على الرغم من أن الانزيم الممتص على السطح أظهر نشاطاً أعلى ، إلا أن ثبات الليباز المغلف كان أفضل بكثير. فعند إعادة استخدام الانزيم المغلف في ZIF-8 حافظ على 83% من النشاط ، مقارنة بنسبة 34% فقط التي حصل عليها الليباز الممتص على السطح في نفس الظروف. وقد تم استخدام التجربة لتحديد المعلمات الحركية لنموذج Ping Pong Bi Bi المعدل، ومقارنتها بما تم الحصول عليه بواسطة نموذج Michaelis Menten. أظهرت النتائج بوضوح أن الركيزة لم تنتشر بعمق في ZIF-8 التي أدت إلى انخفاض نشاط الانزيم المغلف مقارنةً بالمادة الممتصة.

**مفاهيم البحث الرئيسية:** وقود الديزل الحيوي، إطار الزيوليت إيميدازولات، الليباز، الفرق محدود، نموذج انتشار التفاعل.

## **Acknowledgements**

The completion of this study could not have been possible without the expertise of Professor Sulaiman Al Zuhair, my thesis advisor.

I would like to thank Dr. Hussain, Eng. Sami and Eng. Anvar since some of my experimental work would not have been completed without their help.

My Deep sense of gratitude to Allah who help me along the way. In addition, special thanks are extended to my parents and all my family member for their motivation.

## **Dedication**

*To my beloved parents and family*

## Table of Contents

Title .....	i
Declaration of Original Work .....	ii
Copyright .....	iii
Approval of the Master Thesis .....	iv
Abstract .....	vi
Title and Abstract (in Arabic) .....	viii
Acknowledgements .....	ix
Dedication .....	x
Table of Contents .....	xi
List of Tables .....	xiii
List of Figures .....	xiv
List of Abbreviations .....	xv
Chapter 1: Introduction .....	1
1.1 Overview .....	1
1.2 Statement of the Problem .....	2
1.3 Relevant Literature.....	3
1.3.1 Biodiesel.....	3
1.3.2 Biodiesel Feedstock.....	4
1.3.3 Biodiesel Production Processes.....	7
1.3.4 Lipases.....	9
1.3.5 Lipases Immobilization .....	12
1.3.6 Metal-Organic Frameworks .....	20
1.3.7 Kinetics of Encapsulated Enzyme System .....	22
1.4 Aims of the Study .....	27
Chapter 2: Methods .....	28
2.1 Chemicals and Enzyme .....	28
2.2 Synthesis of Lipase Encapsulated in ZIF-8 (L-ZIF) .....	28
2.3 Activity Assay .....	29
2.4 Immobilization Capacity .....	30
2.5 Biodiesel Production .....	31
2.6 Crystal Structure Using XRD.....	32
2.7 Morphology Using SEM .....	32
2.8 Surface Area Analysis and Pore Size Distribution.....	33
2.9 Fourier Transform Infrared (FT-IR).....	33
2.10 Protein Analysis .....	33
Chapter 3: Results .....	34

3.1 Enzyme Activity.....	34
3.2 Immobilization Capacity.....	36
3.3 Crystal Structure .....	37
3.4 Morphology Analysis.....	39
3.5 Pore Size Analysis .....	41
3.6 Fourier Transform Infrared (FT-IR) .....	42
3.7 Different Production Technique of Biodiesel Production.....	43
3.8 Biodiesel Production .....	44
3.8.1 Enzyme Immobilization .....	44
3.8.2 Encapsulated vs Adsorbed L-ZIF.....	45
3.8.3 Biodiesel Production Rate.....	50
3.9 Diffusion-Reaction Model .....	60
Chapter 4: Conclusion.....	67
References .....	68
List of Publications .....	77
Appendix.....	78

## List of Tables

Table 1: Comparison between the three generations of biodiesel feedstock .....	6
Table 2: Advantages and disadvantages of lipases' immobilization .....	13
Table 3: Advantages and disadvantages of immobilization methods .....	16
Table 4: Specific activity of prepared L-ZIF, ZIF-8, Navozym 435 & Soluble Enzyme .....	34
Table 5: Kinetics model parameters of biodiesel production catalyzed by encapsulated lipase in ZIF-8 .....	55
Table 6: Changes in substrate concentration inside ZIF-8 crystal with time .....	63

## List of Figures

Figure 1: Transesterification of triglycerides with alcohol .....	7
Figure 2: Techniques for enzyme immobilization .....	17
Figure 3: Modelled ZIF crystal showing the differential volume element .....	23
Figure 4: Modelled ZIF crystal with different nodes .....	25
Figure 5: Encapsulated enzyme inside the ZIF-8 (sphere).....	26
Figure 6: Synthesis of lipase encapsulated in ZIF-8 (L-ZIF).....	29
Figure 7: XRD of empty ZIF-8 and L-ZIF,.....	38
Figure 8: Scanning Electron Microscopic (SEM) images of empty ZIF-8 and L-ZIF .....	40
Figure 9: N <sub>2</sub> adsorption isotherms of ZIF-8 empty and encapsulated lipase at 77 K.....	42
Figure 10: FT-IR spectra of pure ZIF-8 (without lipase, ZIF-8) and FT-IR spectra L-ZIF. ....	43
Figure 11: Effect of L-ZIF preparation on the activity .....	44
Figure 12: Biodiesel yield after 4 h using L-ZIF as compared to soluble enzyme, Novozym435, empty ZIF-8 and no catalyst, .....	45
Figure 13: Effect of methanol to oil ratio on the biodiesel production yield,.....	46
Figure 14: Percentage recovered activity based on the first cycle, .....	49
Figure 15: Comparison between the experimental and model prediction of the drop in oil concentration, .....	51
Figure 16: Effect of oil concentration on initial rate of biodiesel production and production yield, .....	53
Figure 17: Effect of biodiesel production and production yield of oil concentration on initial rate,.....	57
Figure 18: Effect of temperatures and methanol to oil molar ratio,.....	59
Figure 19: Effect of the water content on FAEEs production .....	60

## List of Abbreviations

BCL	Burkholderia Cepacia Lipase
BET	Brunauer–Emmett–Teller
CO <sub>2</sub>	Carbon Dioxide
CP <sub>s</sub>	Coordination Polymers
D <sub>s</sub>	Diffusivity (cm <sup>2</sup> h <sup>-1</sup> ),
FAMEs	Fatty Acids Methyl Esters
FID	Flame Ionization Detector
FT-IR	Fourier Transform Infrared
GC	Gas Chromatograph
GX	Glucose Oxidase
Hmim	2-Methylimidazole
IUPAC	International Union of Pure and Applied Chemistry
KH <sub>2</sub> PO <sub>4</sub>	Potassium Dihydrogen Phosphate
K <sub>s</sub>	Dissociation Constant of the Substrate
L@ZIF	Lipase at ZIF
MM	Michaelis Menten
MOFs	Metal Organic Frameworks
MPPBB	Modified Ping Pong Bi Bi
Na <sub>2</sub> HPO <sub>4</sub>	Sodium Phosphate Dibasic
NaCl	Sodium Chloride
NaH <sub>2</sub> PO <sub>4</sub> .H <sub>2</sub> O	Sodium Phosphate Monobasic
NaOH	Sodium Hydroxide
NBC	Nanobiocatalyst



PS	Polystyrene
RML	Rhizomucor Miehei
rpm	Revolutions Per Minute
Sb	Bulk of the Solution Per Reactor Volume
SEM	Scanning Electron Microscope
SR	Substrate Concentration at the Surface Per Volume of ZIF Crystals
Sr	Substrate Concentration
u	Initial Rate of Reaction
V <sub>0</sub>	Titrate Volumes in the Lipase and Blank Solutions (ml)
V <sub>1</sub>	Titrate Volumes in the Lipase (ml)
V <sub>max</sub>	Kinetics Parameter (h <sup>-1</sup> )
XRD	X-ray Diffractometer
ZIF	Zeolite Imidazolate Framework-8
Zn(CH <sub>3</sub> CO <sub>2</sub> ) <sub>2</sub>	Zinc Acetate Dehydrate

## Chapter 1: Introduction

### 1.1 Overview

Enzymatic transesterification of triglycerides to produce biodiesel has been gaining increasing attention owing to its advantages over chemical processes. The main advantage is the applicability on a wide range of crude oils, especially those high in free fatty acids, without the need for pretreatment. In addition, the enzymatic processes are environmentally friendly, has lower energy requirements and can offer easy by-product separation (Ismail & Al-Zuhair, 2020). However, the feasibility of the applications of enzymes in any technological process is hindered by the high price of the enzyme. Being catalysts, they are not consumed during the processes in which they are used. Therefore, their repeated use can significantly enhance the economic feasibility of the process. However, soluble enzymes are prone to denaturation and activity loss, and should be stabilized to be utilized in an efficient manner. In their soluble form, enzymes retaining inside the reaction system is difficult and cannot be economically recovered. Besides the negative economic effect of losing the enzyme when it is wasted, they contaminate the product and their removal involve an extra cost. The most common strategy for facilitating easy separation and waste elimination is to immobilize the enzyme on a support matrix.

Enzymes' adsorption onto an insoluble support is a simple method that can allow for high enzyme loading. However, physical adsorption forces are generally weak, leaving the enzyme prone to leaching. In addition, these weak forces do not provide support that may enhance enzyme stability. Chemical adsorption has therefore been suggested to overcome these drawbacks. However, chemical adsorption may affect the enzyme activity. Therefore, in this work, the encapsulation of the enzyme

inside the Zeolite Imidazolate Framework-8 (ZIF-8) matrix has been suggested, which would provide high stability coupled with high activity. Encapsulated lipase in ZIF-8 have shown high thermal stability with 3.2 higher half-life and decreased the deactivation rate as compared to the free enzyme (Nadar & Rathod, 2018). Nevertheless, encapsulating the enzyme inside the Metallic Organic Framework (MOF) adds internal diffusion limitations, which the substrates need to undertake in order to reach the active sites on the enzyme, which are not encountered with surface adsorption. Therefore, it is important not only to determine the activity and stability of immobilized lipase in ZIF, but also to understand the diffusion-reaction process, which is the main objective of this work. To the best of the knowledge of the authors of this work, this is the first attempt to model the diffusion-reaction system of lipase encapsulated inside ZIF-8 for biodiesel production.

## **1.2 Statement of the Problem**

Fossil fuels are essential sources of energy, which meet majority of the current energy demands. However, these sources are non-renewable, and their use causes several global problems. Therefore, research focus has been diverted towards the use of renewable sources of energy that are more environmentally-friendly such as biofuel. In this regard, there are several methods that can be used to prepare the biodiesel. Among them is using immobilized enzyme. Enzyme immobilizations have been used to solve the problems encountered with using the enzyme in a soluble form, which include losing the enzyme with the effluent in a continuous process and product contamination. Adsorption of enzymes onto an insoluble support is a straightforward way for achieving high enzyme loading. Physical adsorption forces, on the other hand, are often minimal, making the enzyme vulnerable to leaching. Furthermore, even mild

pressures do not provide support for enzyme stability. To resolve these disadvantages, chemical adsorption has been recommended. Chemical adsorption, on the other hand, may have an impact on enzyme function. As a result, the encapsulation of the enzyme within the Zeolite Imidazolate Framework-8 (ZIF-8) matrix has been proposed in this work, which would provide great stability and activity. Zeolitic Imidazole Frameworks (ZIFs) which are produced by the metal ions  $Zn^{2+}$  or  $Co^{2+}$ , they consider the best MOF for (Asunción Molina, Gascón-Pérez, Sánchez-Sánchez, & Blanco, 2021). Because the synthesis and encapsulation of other MOF types is too harsh and the encapsulated Wei to be feasible, the expensive enzyme has to be repeatedly used, while maintaining its activity. Using the enzyme in immobilized form allows its easy separation. However, there are other problems encountered with using immobilized enzyme, which are the added mass transfer resistances and the loss of activity. The objective of this work, it is to encapsulate lipase inside ZIF-8 crystals to reduce the leaching likely to be encountered by adsorption methods. A thorough model has been developed to have a better insight into the diffusion-reaction system inside the ZIF-8 pores. To identify the amount of lipase molecular diameter was spread over a ZIF-8 and diffuse into the ZIF-8 (H. F. Liu, Ma, Winter, & Bayer, 2010).

### **1.3 Relevant Literature**

#### **1.3.1 Biodiesel**

Most of the global energy demand is currently met by fossil fuels (Y. Liu et al., 2011). Fossil energy, however, is nonrenewable, and its burning emissions have adverse effects on the environment. Therefore, the dependence on fossil fuels have recently seen a considerable reduction, due to the increasing utilization of various renewable energy sources, reaching 14% of the total energy consumption (Hosseini &

Wahid, 2015). Among the main renewable energy sources are biofuels, which are derived from biomass, such as bio-ethanol, bio-butanol, and biodiesel (Ghadiryantar, Rosentrater, Keyhani, & Omid, 2016). Besides being renewable, biofuels are non-toxic and biodegradable, and their burning emissions have lower particulates and carbon oxides, as compared to fossil fuels. Monoalkylesters are the core components of biodiesel, which is produced by transesterification of triglycerides, which are conventionally found in vegetable oils extracted from oil crops. Because of their numerous advantages and limited commercial production, biodiesel represents approximately 1.5% of global transport fuels.

### **1.3.2 Biodiesel Feedstock**

Feedstock for biodiesel is divided into three generations. The first-generation refers to the oils extracted from crop plants grown exclusively for energy generation (Ghadiryantar et al., 2016). The second generation of biofuels is used cooking oils and waste fats (Branco, Serafim, & Xavier, 2018) (Antizar-Ladislao & Turrion-Gomez, 2008). The third-generation feedstock refers to algal biomass. First generation for biodiesel refers to the extracted oils from crops and oilseed (Antizar-Ladislao & Turrion-Gomez, 2008). The main benefits of using this type of feedstock are the enhancement of agricultural industries and the reduction in greenhouse gas emissions, as a result (Datta, Hossain, & Roy, 2019). However, first-generation feedstock competes with their use as human food on one hand, and they are too expensive of the other biodiesel (Ghadiryantar et al., 2016). Because of that, the first-generation feedstock is rarely considered.

To overcome the food versus energy and high-cost problems of the first-generation feedstock, waste cooking oil and animal fat have been suggested instead,

which are referred to as the second-generation feedstock. Besides their low cost and not competing with food, utilizing second-generation feedstock to produce valuable product, such as biofuels, is a waste minimization and environmentally friendly technique. However, the supply of second-generation feedstock is not consistent and has collection complexities, and therefore it has not been widely used on commercial scale (Datta et al., 2019).

Microalgae oil is considered the third-generation feedstock. Compared to other feedstocks, microalgae have higher growth rates and higher oil productivity (Datta et al., 2019; Mata, Martins, & Caetano, 2010). By photosynthesis, microalgae can fix atmospheric CO<sub>2</sub>, adding the advantage of CO<sub>2</sub> mitigation. In addition, microalgae cultivation for energy production does not have the food vs energy issue. They also do not require agricultural lands and can be grown in saline, or waste, water. On the other hand, microalgae-to-biodiesel process is more expensive than using other sources (Datta et al., 2019; Mata et al., 2010). The Table 1 shows the comparison between the three generations.

Table 1: Comparison between the three generations of biodiesel feedstock

Source	First-generation	Second-generation	Third-generation
	Straight vegetable and crops oils	Waste vegetable oils and waste fats	Microalgae oils
Advantages	<ol style="list-style-type: none"> <li>1. Agricultural industries Enhancement</li> <li>2. Greenhouse gases reduction</li> </ol>	<ol style="list-style-type: none"> <li>1. Cheap</li> <li>2. Using them is considered a waste management</li> </ol>	<ol style="list-style-type: none"> <li>1. Greenhouse gases reduction</li> <li>2. Do not compete with food, and lands used for food plantation</li> <li>3. Could be cultivated in saline and waste waters</li> <li>4. Minimal use of fertilizers</li> </ol>
Disadvantages	<ol style="list-style-type: none"> <li>1. Expensive</li> <li>2. Competition with food, and lands used for food plantation</li> <li>3. High freshwater load</li> <li>4. Fertilizers need</li> </ol>	<ol style="list-style-type: none"> <li>1. Inconsistent supply</li> <li>2. Collection complexities</li> <li>3. Low quantities</li> </ol>	<ol style="list-style-type: none"> <li>1. Relatively expensive process</li> </ol>

### 1.3.3 Biodiesel Production Processes

The most common method for producing biodiesel is transesterification of triglycerides or esterification of fatty acids (Boon-Anuwat, Kiatkittipong, Aiouache, & Assabumrungrat, 2015). As shown in Equation (1) and Figure 1, in transesterification, in the presence of a catalyst, one molecule of tri-glyceride combines with three molecules of an alcohol (such as methanol) to create three molecules of fatty acid alkyl esters and one molecule of glycerol as a by-product (Alex, West, & Ellis, 2008), Whereas, as shown in Equation (2), in esterification, one molecule of fatty acids reacts with one molecule of the alcohol to produce one molecule of fatty acid alkyl ester and one molecule of water as the by-product (Boon-anuwat et al., 2015). Based on the catalyst used, the catalytic processes are classified as homogeneous, heterogeneous and enzymatic processes (Boon-Anuwat et al., 2015).

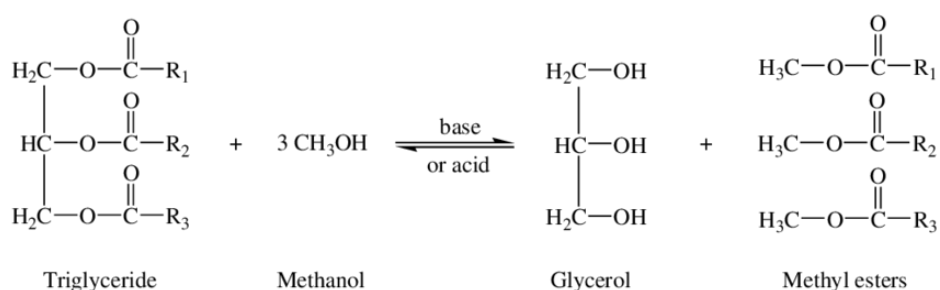
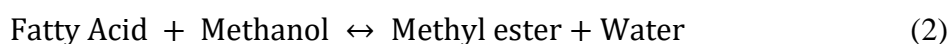


Figure 1: Transesterification of triglycerides with alcohol





### **1.3.3.1 Homogeneous Chemical Catalyzed Processes**

Homogeneous chemical catalyzed processes are divided into base and acid processes. Base catalyzed biodiesel production processes, using for example sodium hydroxide (NaOH), are more common, as they are efficient at relatively low temperatures. However, these processes are sensitive to the free fatty acids content in the feedstock, which reacts with the catalyst in a saponification reaction. This will result in catalyst consumption, yield reduction and downstream separation complexities. Heterogeneous acid catalyst on the other hand, are less sensitive to the free fatty acids, but are much slower and require larger amounts of alcohol, as compared to the base catalyzed process (C. L. B. Reis et al., 2019). In addition, in both chemical catalyzed processes, the product needs to be washed, which results in large wastewater production.

### **1.3.3.2 Heterogeneous Chemical Catalyzed Processes**

Heterogeneous chemical catalyzed processes also use base and acid catalysts, but in a solid heterogeneous form. Although heterogeneous base catalysts are slower than the homogeneous counterparts, they are less sensitive to free fatty acids in the feedstock. In addition, they do not contaminate the product and eliminating the need for the washing step because they do not produce soap as a side product (Ferreira, Menezes, Sampaio, & Batista, 2020). Furthermore, being in a heterogeneous form allows their repeated re-use in a continuous reactor (Lam, Lee, & Mohamed, 2010). The main disadvantage of heterogeneous catalysts is that they are susceptible to deactivation (Lam, Lee, & Mohamed, 2010).

### **1.3.3.3 Enzymatic Catalysed Processes**

Enzymatic processes, using lipase, is a simple process that operates at near ambient temperature and are not sensitive to the fatty acid content in the feedstock. Enzymatic processes, with their advantages and challenges are described in more details in the following sections.

### **1.3.4 Lipases**

Lipases are water soluble enzymes that catalyzes the hydrolysis of ester bonds to form free fatty acids (Mello Bueno, de Oliveira, Castiglioni, Soares Júnior, & Ulhoa, 2015; Reis, Holmberg, Watzke, Leser, & Miller, 2009). They play key role in hydrolysis, esterification, transesterification, interesterification and alcoholysis reaction (Reis et al., 2009).

#### **1.3.4.1 Sources of Lipases**

Lipases are found in various organisms, such as plants, animals, and microbes. In plants, lipases are extracted mainly from the seeds because that contain oils (Filho, Silva, & Guidini, 2019), whereas those from animal sources are extracted from cells that synthesize them or function to digest fats. Animal lipases are not used in commercial purposes because it is challenging to extract them. The third source of lipases are microbial that obtain from bacteria and fungi, which are the most popular and easier to genetically modify for better characteristics and specificities. Fungal lipases, such as from *Candida* yeast, are relatively stable and easy to produce, therefore they are the most commonly used in biotechnological applications.

#### **1.3.4.2 Lipase Catalysed Biodiesel Production**

Lipases hydrolyze the ester bonds in tri-, di-, and monoacylglycerols to catalyze chemical processes (Pizarro & Park, 2003). Like many other catalysts, lipases work by lowering the activation energy of a process or the initial energy input required for it to occur; as a result, the reaction rate increases millions of times (Robinson, 2015). Lipases have various applications in the business, including transformation processes, food and pharmaceutical manufacturing, bioremediation, biofuel cells, and lipases utilized in biomass-derived catalytic conversion technologies (Raveendran et al., 2018). Enzymes usually function at moderate settings, such as ambient temperature and high tension. Enzyme reactions may now be carried out in organic solvents and aqueous conditions to transform nonpolar organic molecules and water-soluble molecules selectively and efficiently. The use of enzymes in commercial chemical synthesis has grown increasingly straightforward and efficient (Ge, Yang, Zhu, Lu, & Liu, 2012).

Biochemists and microbiologists have long recognized enzymes' ability to synthesize chemicals. Over the last decade, it has become clear that using enzymes in organic synthesis poses minimal difficulties (Winkler, Schrittwieser, & Kroutil, 2021). Consequently, enzymes can be used in raw or complex transformations without using inducers or inhibitors, which are widely used in enantio- and regioselective organic syntheses. High selectivity also allows for valuable reactions with little by-products, making enzymes a more ecologically sustainable alternative to classical chemical synthesis in the food and pharmaceutical sectors. On difficult substrates, a high reaction selectivity is required (Mu et al., 2020). Enzyme selection is now becoming a prerequisite for the chemical industry to improve different methods. The synthesis

of sophisticated compounds and polymers has benefited from recent advances in enzymatic catalysis.

Immobilized lipase from *Candida* sp. on an inexpensive cotton membrane was used for transesterifying fats and oils. The conversion ratio of salad oil to biodiesel might surpass 96% under ideal reaction circumstances (Tan, Nie, & Wang, 2006). Lipases have several advantages, the first of which is enhanced solubility Tan of hydrophobic substrates. Ease of enzyme immobilization, recovery, and reusability without immobilization by sample absorption onto the nonporous platform. Water-dependent side reactions are suppressed, and the enzyme has the potential to be employed directly in a chemical process (Kumar, Dhar, Kanwar, & Arora, 2016).

In certain cases, free enzymes were used in solution, but using enzymes in an immobilized state is preferable in many functional applications. Enzyme re-using is essential for many bioprocesses because enzymes are costly. Soluble enzymes may contaminate a substance and removing them can require additional purification costs (Cao et al., 2016).

#### **1.3.4.3 Other Applications of Lipase**

Lipases are widely utilized to refine fats and oils, detergents and degreasing formulations, food processing, fine chemical and pharmaceutical synthesis, paper production, and cosmetic and pharmaceutical production (Kazlauskas & Bornscheuer, 2008). Lipase is commonly used in commercial detergent and domestic cleaners because of its distinctive properties and ability to break down fats. Because of its ability to survive the rigors of washing (Cardenas et al., 2001; Sharma, Chisti, & Banerjee, 2001). Moreover, the lipases used in food and beverages, including dairy products, baked goods, fruit and vegetable processing, as well as its use in fermentation

and animal feed (Sharma et al., 2001). Including it is used in biofuel production, pharmaceutical industry, textile processing, and many other uses due to its distinct properties (Guerrand, 2017).

### **1.3.5 Lipases Immobilization**

In recent years, enzyme immobilization on support materials has gained popularity (Misson, Zhang, & Jin, 2015). Lipase's immobilization is characterized by the combination of the physical and chemical properties of the carrier and the lipase's selectivity, stabilization, and kinetic properties, which enhance the stability of the lipase function. For enzyme immobilization, various methods are used, but the industry often prefers convenient and cost-effective methods. Chemical immobilization (covalent binding and cross-linking) and physical immobilization (adsorption or physical entrapment) are the two most widely used techniques. (Filho et al., 2019). The main objective of immobilized is to create a stable biocatalyst that can be reused multiple times with negligible loss of operational activity (Homaei, Sariri, Vianello, & Stevanato, 2013). Table 2 summarized the advantages and disadvantages if enzyme immobilization.

Table 2: Advantages and disadvantages of lipases' immobilization

Advantages	Disadvantages
Simple biocatalyst isolation	Lower enzyme activity than native enzymes
Lower downstream processing costs Multiple biocatalysts uses (recycling)	Higher prices for carriers and immobilization
Improved stability	Lower reaction speeds than native enzymes
Co-immobilization of other enzymes is feasible using fixed bed or batch reactors without using a membrane to separate enzyme from substance.	Membrane Fouling
	Disposal of the depleted immobilized enzyme (incineration)

The use of enzymes depends on the price of the enzyme and the applications involved (Basso & Serban, 2019). An insoluble enzyme is a heterogeneous catalyst used in different process formats to recover and re-use it and its ability. An enzyme's immobilization is converting the enzyme from soluble and insoluble to more stable, combining the selectivity, stability, and kinetic of that enzyme with the physical and chemical properties of the carrier in a specialized formulation (Homaei et al., 2013).

#### **1.3.5.1 Need for Immobilization.**

The purpose of enzyme immobilization is to make biocatalytic process more economics by allowing the enzyme to be easily separated and reused for several cycles (Guzik, Hupert-Kocurek, & Wojcieszynska, 2014; Mokhtar, Rahman, Noor, Mohd Shariff, & Mohamad Ali, 2020). In addition, immobilization can help enzymes perform better under various reaction conditions (acidic, alkaline, organic solvents,

and high temperatures), making it suitable for industrial chemical synthesis (Papamichael & Stergiou, 2020). A series of steps must be taken to produce immobilized enzyme, beginning with selecting the support material and testing the immobilization conditions to achieve the optimal state. The evaluation of laboratory conditions during the process to increase operating performance. The catalytic activities of the biocatalyst generated are characterized under operating conditions (Dias Gomes & Woodley, 2019).

### **1.3.5.2 Challenges of Using Immobilized Lipase and Proposed Solutions**

The loss of catalytic activity, mainly when the enzymes are operating on macromolecular substrates, is one of the most severe issues connected with the usage of immobilized enzymes. In addition, enzyme's activity could be restricted to the substrate's visible surface groups (Boundy, Smiley, Swanson, & Hofreiter, 1976). The normal pattern of products produced from the macromolecular substrate may change due to the steric limitation. Utilizing supports made up of networks of isolated macromolecular chains, carefully selecting the enzyme residues involved in immobilization, and using hydrophilic and inert spacer arms are the most popular techniques for resolving the steric problem. Immobilization-induced changes in catalytic properties could be attributed to changes in the protein's three-dimensional structure produced by the enzyme's attachment to the matrix. These effects have been verified and used to a lesser extent for a small number of enzyme systems (Brena, González-Pombo, & Batista-Viera, 2013).

### **1.3.5.3 Method of Immobilization**

Enzyme immobilization can be accomplished in various methods, but the industry often favors cost-effective and straightforward approaches (Homaei et al.,

2013). Physical approaches typically show weak and noncovalent enzyme-support interactions such as hydrogen bonding, hydrophobic interactions, van der Waals forces, and ionic binding such as adsorption or physical entrapment (Filho et al., 2019). Covalent binding and cross-linking are chemical processes that include creating covalent bonds between enzymes and support bonds like ether, amide, or carbamate (Reis et al., 2009). Figure 2 shows graphical presentation of the common immobilization techniques, and Table 3 compares between them.



Table 3: Advantages and disadvantages of immobilization methods

Immobilization method	Advantages	Disadvantages
Physical adsorption	<ul style="list-style-type: none"> <li>- Very easy to adsorb enzymes to matrices.</li> <li>- Separating and purifying enzymes when immobilized is possible.</li> <li>- Enzymes are not deactivated.</li> </ul>	<ul style="list-style-type: none"> <li>- Immobilization performance is limited.</li> <li>- Sensitive to pH, ionic strength, and temperature of the solution.</li> <li>- Due to the poor interactive force, the amount of enzymes is low.</li> </ul>
Chemical binding	<ul style="list-style-type: none"> <li>- Variety of organic linkers available.</li> <li>- Strong binding force</li> </ul>	<ul style="list-style-type: none"> <li>- Important variations in the enzyme's active site, which then distorts or makes the active site inaccessible.</li> <li>- Due to the additional reagents used, the cost is high.</li> <li>- The enzyme loading is poor.</li> </ul>
Entrapment or encapsulation	<ul style="list-style-type: none"> <li>- Enzyme molecules are kept in place</li> <li>- Enzyme molecules are free to jump about within carriers.</li> </ul>	<ul style="list-style-type: none"> <li>- Experimentation is a difficult process.</li> <li>- Reduce the rate at which reactants and products diffuse.</li> <li>- Entrapped enzymes cannot be used with high-molecular-weight substrates due to the difficulties big molecules have reaching the catalytic sites of entrapped enzymes.</li> </ul>
Cross-linking	<ul style="list-style-type: none"> <li>- Shelf life and organizational reliability have been improved.</li> <li>- Recoverable and re-usable</li> <li>- In aqueous media, it is resistant to leaching.</li> </ul>	<ul style="list-style-type: none"> <li>- The enzyme's versatility is being lost.</li> <li>- Reduce the rate at which reactants and products diffuse.</li> </ul>

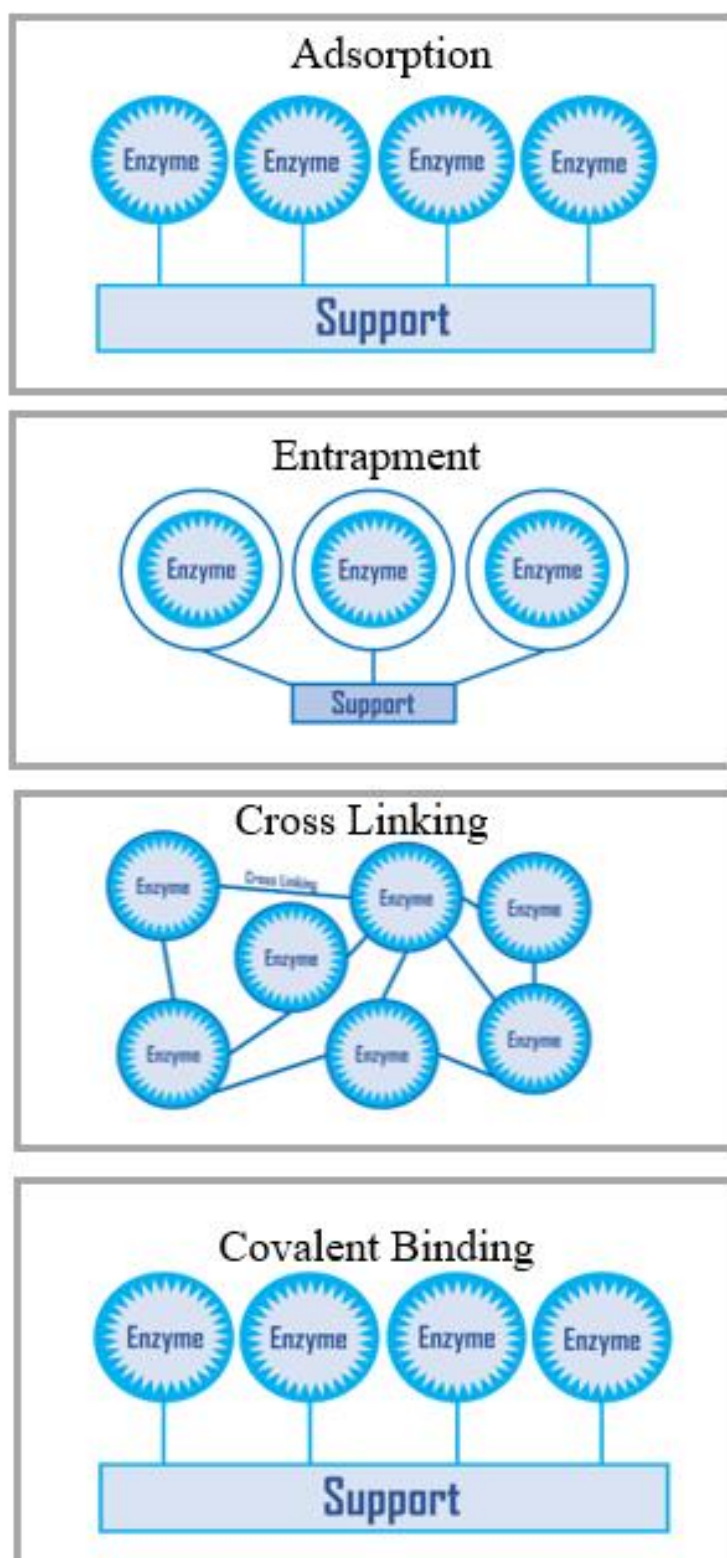


Figure 2: Techniques for enzyme immobilization

### **1.3.5.3.1 Adsorption**

Physical adsorption is possibly the easiest enzyme immobilization technique, which requires a physical contact between the adsorbent surface and the enzyme to create van der Waals, ionic or hydrophobic interaction (Jesionowski, Zdarta, & Krajewska, 2014; Marchetti, Miguel, & Errazu, 2007; Mohamad, Marzuki, Buang, Huyop, & Wahab, 2015; Wahab, Elias, Abdullah, & Ghoshal, 2020). To enhance the lipases' adsorption potential on the support, specific parameters, such as pH, ion power, temperature, initial protein loading, and contact time need to be specified and adsorption kinetics, mechanism, and thermodynamics need to be understood (Batool, Akbar, Iqbal, Noreen, & Bukhari, 2018). Generally, lipases have a high level of hydrophobic activity, and they spontaneously adsorb from aqueous solutions to hydrophobic surfaces faster than most other proteins (Mohamad et al., 2015).

### **1.3.5.3.2 Covalent Binding**

Covalent bonding is the traditional method of permanent enzyme immobilization, which consists of forming covalent bonds between the enzyme and the support material (Homaei et al., 2013). These associations include side-chain amino acids such as lysine, cysteine, aspartic and glutamic acids and many functional groups such as carboxyl group, amino group, epoxy group, indole group, phenolic group, sulfhydryl group, thiol group, imidazole group, and hydroxyl group, which are not necessary for the catalytic activity of the enzyme. Covalent immobilization has an advantage over adsorption immobilization in that the enzyme will stay on help under tight circumstances and may also be incorporated in the reaction media (Homaei et al., 2013). Covalent bonding creates a strong support-enzyme link that ensures the enzyme is strongly fixed. It prevents enzyme leach into the reaction media, which allows for

more re-use cycles (Mohamad et al., 2015; Nguyen & Kim, 2017). The covalent bonding also allows immobilized lipase unfold/refold reactivation without the risk of lipase desorption (Çakmakçi, Muhsir, & Demir, 2017). However, with continuous reactivation cycles, the recovery of enzyme activity reduces, and the exact identical structure of the enzyme is not achieved after each refolding session (Rueda et al., 2015). In general, covalently immobilized enzymes should be employed in reaction media in which the enzyme is prone to leaching, such as in aqueous solutions (C. L. B. Reis et al., 2019). In addition, they can be used under harsh condition, as the covalent bonds are strong enough to hold the enzyme-bound, reducing conformational flexibility and thermal vibrations. However, the main challenge for this method is the chemical alteration to which the enzyme is submitted, resulting in a drop in the activity (Vieille & Zeikus, 2001).

#### **1.3.5.3.3 Entrapment**

Entrapment is another permanent enzyme immobilization strategy, similar to covalent bonding, as long as the aid used is completely insoluble throughout the reaction media (Homaei et al., 2013; Wahab et al., 2020). In this process, the support is not prefabricated, but rather produced in the existence of the enzymes that been captured within the produced matrix (Homaei et al., 2013). The method combines the advantage of physical adsorption in which the enzyme structure is not chemically altered, with that of the chemical adsorption in which leaching is reduced (Homaei et al., 2013). The conditions of support for the development of the enzyme must also be consistent with the viability of the enzyme used in order to prevent premature denaturation of the biocatalyst (H. F. Liu et al., 2010). The main disadvantage of this immobilization technique is the high internal mass transfer resistances. The substrate

molecules need to diffuse through the support pores to reach the enzyme, which requires higher concentrations to increase the diffusion driving force (Robinson, 2015). Therefore, it is essential to thoroughly study the support's morphology and porosity.

### **1.3.6 Metal-Organic Frameworks**

Coordination Polymers (CPs) are stiff materials made up of a network of metal ions that are covalently bonded to multiple organic molecules (Engel & Scott, 2020). This description includes a broad range of materials comprising metals and organic molecules with a variety of properties, including crystalline and amorphous solids, porous and nonporous solids, and porous and nonporous liquids (Corma, García, & Llabrés i Xamena, 2010). This research will concentrate on MOFs, which are crystalline and porous compounds with heavy metal-ligand interactions. Over the last 15 years, the Metal-Organic Framework (MOF) industry has expanded rapidly. Metal-Organic Frameworks (MOFs) have been created by combining two separate linkers with the same topology in a single batch or sequentially to produce coordination copolymers with either a uniformly mixed or a core-shell linker composition (Koh, Wong-Foy, & Matzger, 2009). Organic linkers and metal ions are the two primary components of MOFs. Because of the wide range of linkers and metal ions that can be used, as well as the fact that the elements of their assembly can be crystallized and extensively identified, this class of materials has achieved widespread acceptance.

The pore size, form, dimensionality, and chemical environment of MOFs can be precisely regulated by carefully choosing their building blocks (metal and organic linkers) and how they are linked. As molecular sieves, this allows for the selection of molecules that can diffuse through the pores. They can modify host-guest interactions

and the transition states produced for the pores' reactions when adsorbing molecules. Shape-selective and molecular sieve properties can be found in these coordination polymers. The potential to adjust the substance for specific uses by altering and functionalizing the organic ligand using conventional organic chemistry techniques (Corma et al., 2010).

#### **1.3.6.1 Properties and Applications of MOF**

Metal organic frameworks have several benefits that have aided adoption, including their huge surface area, porosity, ease of pore fixing, and surface modification (Nadar & Rathod, 2018). Owing to their unique structures and functions, MOFs potential applications have been evaluated in various fields, such as gas adsorption/separation, catalysis, sensors, drug delivery, magnetic materials, and optical devices (Chen et al., 2020).

#### **1.3.6.2 Synthesis of MOFs**

Metal Organic Frameworks (MOFs) can take on a crystalline structure in various ways, depending on the type of liquid solvent, the components utilized, and the process used to combine them. Metals and ligands are frequently mixed in a coordinated manner to produce structure crystals of MOFs. Some of the most well-known metals are metal nitrates, sulfates, or acetates, and organic components such as Mono-, di-, tri-, and tetracarboxylic acids are the common polar organic solvents, such as triethylamine or amide (diethylformamide, dimethylformamide) (Czaja, Trukhan, & Müller, 2009). MOFs are generally produced under a moderate temperature and stirring is required once the organic and inorganic components have been combined. Sometimes, additional auxiliary molecules are needed (Czaja et al., 2009).

### 1.3.7 Kinetics of Encapsulated Enzyme System

The kinetic behavior of an encapsulated enzyme in ZIF differs significantly from that of the enzyme in free form. Substrate molecules diffuse through the surrounding layer to reach the MOF surface and then diffuse within the pores to encounter the enzyme and react. In internal diffusion limited system, as the one used in this work, in which effective turbulent are forced by thorough mixing, the concentration of the substrate at the surface of the ZIF is effectively equal to that in the bulk. The mixing in the reaction system, however, have no effect on the internal diffusion of the substrate within the pores of the ZIF-8 crystals. To analyze the effect of internal diffusional on the reaction catalyzed by lipase encapsulated inside ZIF-8, the crystal was modeled by a sphere, as shown in Figure 3, and the following assumptions were used to simplify the model: immobilized enzyme is uniformly distributed throughout the length of the pores of the ZIF-8, the tortuosity is unity, isothermal condition, diffusion of substrate obeys Fick's law with constant effective diffusivity throughout the ZIF pores, neglected external diffusional resistance (i.e. the substrate concentration at the surface per volume of ZIF crystals,  $[S_R]$ , is equivalent to that in the bulk of the solution per reactor volume,  $[S_b]$ ). The two concentrations, however, have different unites, where in the former is per volume of crystals and the latter is per volume of reaction mixture. Considering the differential volume element shown in Figure 5.

Amount of substrate diffused into the slice from the outside of the slice, within  $\delta t$ :

$$D_s [4\pi(r + \delta r)^2] \left. \frac{\partial [S_r]^t}{\partial r} \right|_{r+\delta r} \delta t \quad (1)$$

Amount of substrate diffused out of that slice towards the interior of the particle, within  $\delta t$ :

$$D_s [4\pi r^2] \left. \frac{\partial [S_r]^t}{\partial r} \right|_r \delta t \quad (2)$$

Amount of substrate consumed within the slice within  $\delta t$ , assuming a first order kinetics:

$$V_{\max} [S_r]^t \frac{4}{3} [\pi (r + \delta r)^3 - r^3] \delta t \quad (3)$$

Accumulated amount of substrate within the slice:

$$([S_r]^{t+\delta t} - [S_r]^t) \frac{4}{3} [\pi (r + \delta r)^3 - r^3] \quad (4)$$

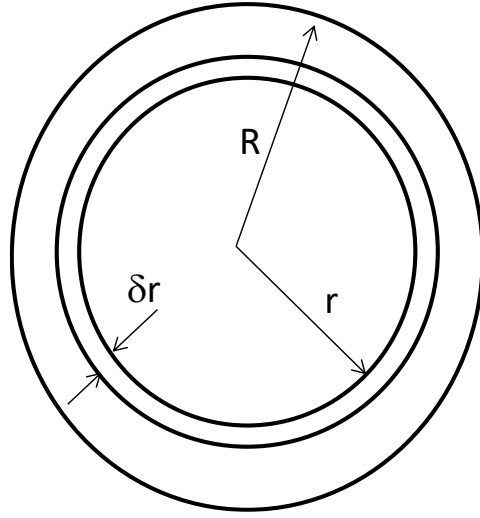


Figure 3: Modelled ZIF crystal showing the differential volume element

Combining them into the overall material balance equation:

$$D_s [4\pi (r + \delta r)^2] \left. \frac{\partial [S_r]^t}{\partial r} \right|_{r+\delta r} \delta t - D_s [4\pi r^2] \left. \frac{\partial [S_r]^t}{\partial r} \right|_r \delta t - V_{\max} [S_r]^t \frac{4}{3} [\pi (r + \delta r)^3 - r^3] \delta t = ([S_r]^{t+\delta t} - [S_r]^t) \frac{4}{3} [\pi (r + \delta r)^3 - r^3] \quad (5)$$

Diving by  $4\pi r \delta r \delta t$  and eliminated the insignificant terms:

$$D_s \frac{\left. \frac{\partial [S_r]^t}{\partial r} \right|_{r+\delta r} - \left. \frac{\partial [S_r]^t}{\partial r} \right|_r}{\delta r} + D_s \frac{2}{r} \frac{\partial [S_r]^t}{\partial r} - V_{\max} [S_r]^t = \frac{([S_r]^{t+\delta t} - [S_r]^t)}{\delta t} \quad (6)$$



Taking the limit as  $\delta r$  and  $\delta t$  approach zero:

$$D_s \frac{\partial^2 [S_r]}{\partial r^2} + D_s \frac{2}{r} \frac{\partial [S_r]}{\partial r} - V_{\max} [S_r] = \frac{\partial [S_r]}{\partial t} \quad (7)$$

Where,  $D_s$  is the diffusivity ( $\text{cm}^2 \text{h}^{-1}$ ),  $V_{\max}$  is the kinetics parameter ( $\text{h}^{-1}$ ),  $[S_r]$  is the substrate concentration inside the ZIF-8 particle at radius  $r$  ( $\text{mg cm}^{-3}$ ), which is the substrate concentration per volume of ZIF-8 crystals. Dividing the radius of the crystal into several nodes and the time into several time intervals, as shown in Figure 3, the material balance (Equation 7) can be represented by Equation (8).

$$D_s \left[ \frac{S_{r,i+1}^n - 2S_{r,i}^n + S_{r,i-1}^n}{\Delta r^2} \right] + D_s \frac{2}{r} \left[ \frac{S_{r,i+1}^n - S_{r,i}^n}{\Delta r} \right] - V_{\max} S_i^n = \left[ \frac{S_{r,i}^{n+1} - S_{r,i}^n}{\Delta t} \right] \quad (8)$$

Equation (8) can then be rearranged to present  $S_{r,i}^{n+1}$  explicitly in terms of the other previous time values, as given in Equation (9).

$$S_{r,i}^{n+1} = S_{r,i+1}^n \Delta t \left( \frac{D_s}{\Delta r^2} + \frac{2D_s}{r\Delta r} \right) + D_s \Delta t \frac{S_{r,i-1}^n}{\Delta r^2} - S_{r,i}^n \left[ \Delta t \left( \frac{2D_s}{\Delta r^2} + \frac{2D_s}{r\Delta r} + V_{\max} \right) + 1 \right] \quad (9)$$

Using a first order kinetic model with no inhibition is used; the partial differential equation that describes the diffusion-reaction of the substrate inside ZIF-8 pores, shown in Equation (7) was developed. The first order kinetics with no inhibition can be replaced with a more detailed model in the future for a more accurate presentation of the reaction.

As mentioned earlier, this concentration has a different unit than that of the bulk concentration, which is per volume of reaction mixture. The partial differential equation (Equation 7) can be solved using the initial and boundary conditions given in Equations (10-13) as shown in Figure 4.

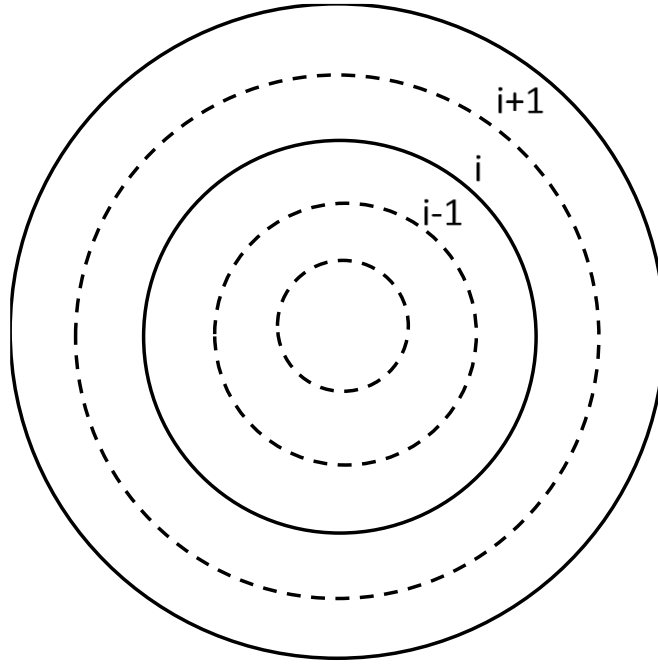


Figure 4: Modelled ZIF crystal with different nodes

Initially the ZIF pores are free of substrate

$$\text{I.C.: at } t = 0 \quad [S_r] = 0 \quad (10)$$

Due to symmetry, at the center of the ZIF:

$$\text{B.C.1: at } r = 0 \quad \frac{d[S_r]}{dr} = 0 \quad (11)$$

Drop in bulk concentration should equal the amount diffused into the ZIF at the surface

$$\text{B.C.2: at } r = R \quad \frac{3m_c}{R\rho_c} D_s \frac{\partial[S_r]}{\partial r} = V_r \frac{\partial[S_b]}{\partial t} \quad (12)$$

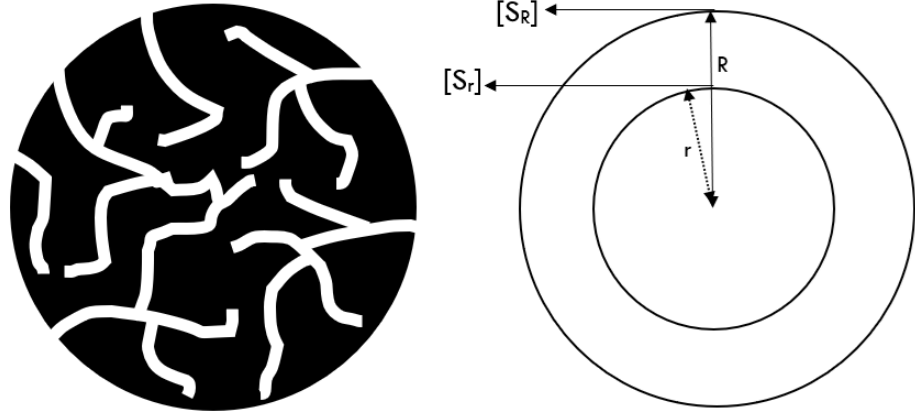


Figure 5: Encapsulated enzyme inside the ZIF-8 (sphere)

To solve this system, the partial differential equations with its initial and boundary conditions are presented using numerical finite difference, in which the future concentration,  $S_i^{n+1}$ , is explicitly presented in terms of the other previous time values, as given in Equations (13-16). The derivation of Equation (13) is found in the Supplementary Document.

$$S_{r,i}^{n+1} = S_{r,i+1}^n \Delta t \left( \frac{D_s}{\Delta r^2} + \frac{2D_s}{r\Delta r} \right) + D_s \Delta t \frac{S_{r,i-1}^n}{\Delta r^2} - S_{r,i}^n \left[ \Delta t \left( \frac{2D_s}{\Delta r^2} + \frac{2D_s}{r\Delta r} + V_{\max} \right) + 1 \right] \quad (13)$$

$$\text{I.C.: at } t = 0 \quad S_i = 0 \quad (14)$$

$$\text{B.C.1: at } r = 0 \quad S_0 = S_1 \quad (15)$$

$$\text{At } r = R \quad S_b^{n+1} = S_b^n - \frac{3m_c D_s \Delta t}{V_r R \rho_c \Delta r} (S_R^n - S_{R-1}^n) \quad (16)$$

Where,  $S$  is the substrate concentration in the ZIF, subscripts  $i$ ,  $R$  and  $b$  represents the node number, the surface concentration and the bulk concentration, and the superscript  $n$  represents the time. As mentioned earlier,  $S_i$  is the substrate concentration per volume of ZIF crystals, whereas  $S_b$  is the bulk concentration per volume of the reaction system.

#### **1.4 Aims of the Study**

The Aim of this thesis is to study biodiesel production from vegetable oil using lipase encapsulated inside ZIF-8 crystals. To achieve this, the following tasks have been performed:

1. To prepare lipase-ZIF and empty ZIF-8 and study its surface and porosity characteristics.
2. To study the effects of methanol:oil ratio, enzyme loading and temperature on the activity of lipase-ZIF used in biodiesel production.
3. To identify the optimum conditions to produce biodiesel and determine and test the reusability of L-ZIF.
4. To study the kinetics of the reaction.

## Chapter 2: Methods

### 2.1 Chemicals and Enzyme

Soluble lipase from Eversa Transform 2.0 was a kind gift from Novozymes, Denmark. The enzymes were stored at 4°C according to supplier's instructions. 2-Methylimidazole and zinc acetate were obtained from Merck, USA. Olive oil, used as a substrate oil, was purchased from local market. Bradford reagent for protein detection and all other chemicals were of analytical grade and purchased from Merck, USA. Hydrogen, zero air (ultra-pure), helium, carbon dioxide, and nitrogen were supplied by Sharjah Oxygen Company, UAE. The sodium phosphate dibasic, sodium phosphate monobasic,  $\text{KH}_2\text{PO}_4$ ,  $\text{NaCl}$ , phenolphthalein indicator, n-hexane, methanol and all other chemicals were purchased from Sigma Aldrich.

### 2.2 Synthesis of Lipase Encapsulated in ZIF-8 (L-ZIF)

Enzyme solution was prepared by diluting 1 ml of enzyme stock solution (2.36 U/ml) in 4 ml of distilled water. The buffer solution was prepared as described by (Mohan, 2006) by mixing 11.54 ml of sodium phosphate dibasic ( $\text{Na}_2\text{HPO}_4$ ) solution (0.142 g/ml) with 8.46 ml of sodium phosphate monobasic ( $\text{NaH}_2\text{PO}_4 \cdot \text{H}_2\text{O}$ ) solution (0.138 g/ml). The total volume was brought to 200 ml by adding 180 ml of distilled water.

A procedure similar to that described by Nadar and Rathod (2018) was used to prepare lipase encapsulated in ZIF-8 (L-ZIF). Briefly as Figure 6 shows, one ml of zinc acetate solution (1.33 mmol/ml) was mixed with 1 ml of enzyme in distilled water. To that, 4 ml of 2-methylimidazole (3.325 mmol/ml) were added, and the mixture was agitated at room temperature for 10 s using stirrer (CB162, UK). The solution was then

left for 24 h at room temperature without stirring and after that, the formed precipitate was separated by centrifugation (IEC CL31 Multispeed, Japan) at 6000 rpm for 10 min. The collected precipitate (i.e., L-ZIF) was washed five times in buffer solution to remove unreacted precursors then dry it with vacuum drier (Dihan Scientific Oven, Korean) at 30°C, -0.5 bar for 24 h. The amount of collected L@ZIF was roughly 0.45 g, and its activity was determined as described in Section 2.3.

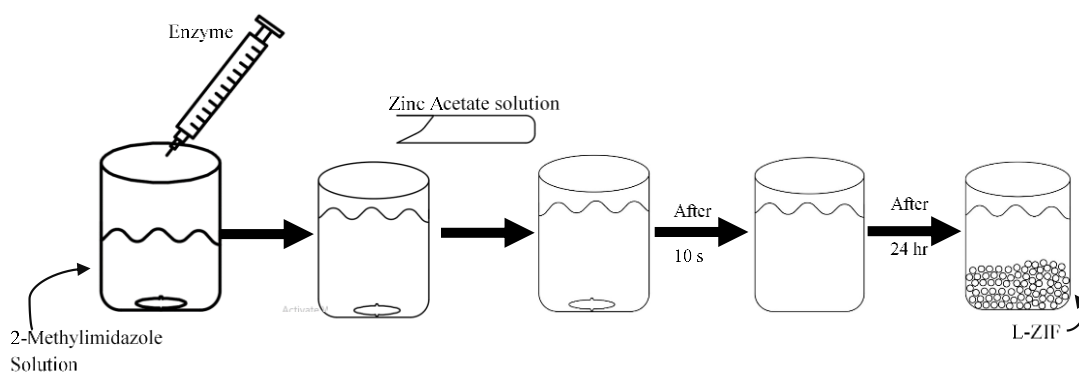


Figure 6: Synthesis of lipase encapsulated in ZIF-8 (L-ZIF)

### 2.3 Activity Assay

For a better estimation of the activity of the free and immobilized enzyme, the hydrolysis assay of the same oil, namely olive oil, used in the biodiesel production experiment was also used in the activity determination. Emulsifying reagent was prepared by dissolving 0.04 g  $\text{KH}_2\text{PO}_4$  and 1.79 g  $\text{NaCl}$  in a 54 ml of glycerol with 40 ml demineralized water. The mixture was agitated by using magnetic stirrer (CB162, UK), and 0.6 g Gum Arabic were added slowly until a homogenized mixture is formed. Then, demineralized water was added to make up the volume of the mixture to 100 ml. The substrate emulsion was prepared by mixing 20 ml of emulsifying reagent with 2

ml of olive oil and 98 ml of demineralized water using a mixer at its highest speed. Once the emulsion was stabilized, 1 ml of diluted enzyme in buffer solution was added to 6.5 ml of oil emulsion to initiate the hydrolysis reaction. When immobilized enzyme was used, the enzyme solution was replaced with 0.1 g of the immobilized enzyme. The mixture was incubated at 40°C for 30 min. After that, two drops of phenolphthalein indicator were added, and the solution was titrated using 0.5 mM NaOH until the color changes. An additional blank test was done following the same procedure, except replacing the 1 ml enzyme solution with 1 ml of distilled water. The volume of NaOH needed to neutralize the produced fatty acids was recorded and used to determine the specific activity of the enzyme using Equation (17).

$$\text{Specific activity} = \frac{(V_1 - V_0) \times M_{\text{NaOH}} \times 10^3}{V \times 0.5 \text{ h}} \quad (17)$$

Where,  $V_1$  and  $V_0$  are the titrate volumes in the lipase and blank solutions (ml), respectively,  $M_{\text{NaOH}}$  is the molarity of NaOH (M) used, 103 is a conversion factor 'from milli-equivalent to micro-equivalent, and  $V$  is the volume of enzyme solution used (ml). With immobilized lipase,  $V$  in Equation (17) is replaced with the weight of the immobilized enzyme used.

## 2.4 Immobilization Capacity

To eliminate the effect of mass transfer on the activity of encapsulated enzyme, protein content was used to determine the immobilization capacity and to have a consistent basis for results comparisons. To determine the adsorption capacity of the ZIF-8, 1.27 mg of already prepared empty ZIF-8, activated in a vacuum oven, was soaked in 10 ml of lipase solution, containing 4.67 mg protein per ml, for 6 h under continuous stirring using magnetic stirrer. The protein concentration was measured at

time zero and at the end of the experiment, after the ZIF-8 was separated by centrifugation, following by vacuum filtration. The background used in the spectrophotometer was distilled water. To determine the encapsulated protein in ZIF-8, the enzyme solution was added with the precursors prior to crystallization, as described in Section 2.10. The proteins concentration before encapsulation and in the supernatant after the removal of the produced crystals were measured. In this case, the background was the initial solution used to prepare the empty ZIF, consisting of same precursors mixture, but with 1 ml of distilled water, instead of 1 ml of the enzyme solution used in the preparation of the encapsulated lipase. The encapsulated lipase in ZIF-8 was determined from the difference of the two protein concentrations multiplied by the sample volume and divided by the amount of ZIF-8 used.

## **2.5 Biodiesel Production**

In each experiment, 1 g of olive oil was mixed with 0.57 ml methanol, at a molar ratio of 1:12 between the oil and methanol, 1 ml of n-hexane and 0.5 ml of diluted enzyme solution, or 0.2 g of immobilized enzyme (L-ZIF). The organic solvent, n-hexane, was added to improve the activity of immobilized enzymes and reduce the leaching (Klibanov, 2001; Su & Wei, 2008). It was reported that by the addition of n-hexane to the reaction medium, enzymatic biodiesel production yield increased to 95%, as compared to only 19% in solvent free under the same reaction conditions (Nelson, Foglia, & Marmer, 1996). The reaction mixture was placed in a water bath-shaker (Maxturdy-30; DAIHAN Scientific, Korea) at 40°C and 250 rpm. After 4 h of incubation, 5 ml of n-hexane were added to the sample and the mixture was centrifuged at 6000 rpm for 3 min to separate two layers. 1 ml of the upper organic layer was withdrawn, and the volume was completed to 10 ml using n-hexane and was sent for



Gas Chromatograph (GC) which is appear in Appendix Figure A-1 (Shimadzu, GC-2010, Japan) for Fatty Acids Methyl Esters (FAMES) analysis. The GC was attached to a Flame Ionization Detector (FID) and a SP-2560 capillary column. The carrier gas used was helium at a flow rate of 40 ml/min. The temperature of the GC oven was set at 195°C for 4 min and then heated to 240°C at a rate of 5°C per min and maintain for 12 min. The GC was calibrated using a solution of known concentrations of FAMES standards. A sample of 1  $\mu\text{m}$  was injected into the column through 0.45  $\mu\text{m}$  filter. The biodiesel yield was determined from the measured FAMES as given by Equation (18).

$$\text{Biodiesel yield (\%)} = \frac{W_e}{W_o} \times 100 \% \quad (38)$$

Where,  $W_e$  is the measured weight of produced FAMES, as determined by the GC, and  $W_o$  is the weight of oil used.

## 2.6 Crystal Structure Using XRD

X-Ray Diffractometer analyzer (XRD system, XPERT-3 Philips, Netherlands) was used to analyze the crystal structure of the prepared ZIF-8 samples. The X-ray analysis was done using copper as an anode material at 40 mA and 45 kV. The measurement peaks range were between  $5^\circ < 2\theta < 50^\circ$  and the step size was 0.013. X-Ray was measured for encapsulated L-ZIF and compared to that of the empty ZIF-8.

## 2.7 Morphology Using SEM

Scanning Electron Microscope (SEM) (JCM-5000 NeoScope, Japan) images were used to study the morphology of ZIF-8 and encapsulated L-ZIF as shows in the Appendix figure A-2. Prior to analyses, the samples were cleaned then coated with gold using Auto Fine Coater (JFC-1600, Japan), to increase the conductivity of the

specimen. Electron beams from the SEM are collide with ZIF-8 samples to generate the morphology images.

## **2.8 Surface Area Analysis and Pore Size Distribution**

The surface area was measured by used a gas physisorption instrument (TriStar II 3020 Analyzer, Japan) which used a liquid nitrogen to obtain the surface area of the ZIF-8 and encapsulated L-ZIF. During the measuring of the surface area the temperature was kept at 77 K.

## **2.9 Fourier Transform Infrared (FT-IR)**

Fourier transform infrared (FT-IR) spectra were obtain using an infrared spectrometer as shows in the Appendix Figure A-3 (JASCO FT/IR-4700, Japan). The FT-IR used as the lipase can absorb infrared wavelengths because of the presence of the bond vibrations (Y. Liu et al., 2011). The FT-IR for ZIF-8 and L-ZIF were obtained in the region of 600 – 4000  $\text{cm}^{-1}$ .

## **2.10 Protein Analysis**

The protein concentration in a sample was measured by adding a Bradford reagent and measuring the optical absorption at 595 nm using a spectrophotometer (BMG SPECTROstar, Germany). The concentration was then determined by comparing the measured optical density to a calibration curve prepared using serial dilutions of known standard protein, albumin, concentration.

## Chapter 3: Results

### 3.1 Enzyme Activity

As mentioned in Section 2.3, the same substrate, olive oil, used in the biodiesel production experiment, was also used in the activity determination to give a more realistic evaluation. The catalytic activity of the prepared encapsulated L-ZIF was measured and compared to that of the empty ZIF-8 and the Eversa Transform 2.0 lipase solution used in its preparation. In addition, the activity Novozyme435, which is a commercially available *Candida antarctica* lipase immobilized on a resin commonly used in biodiesel production (Moreira et al., 2020), was also measured. The comparison is shown in Table 4, in which one unit enzyme activity is defined as the amount of the enzyme that produces 1  $\mu\text{mol}$  of fatty acids per hour.

Table 4: Specific activity of prepared L-ZIF, ZIF-8, Navozym 435 & Soluble Enzyme

Type of enzyme	Specific activity	Unit
Soluble enzyme	$236 \pm 1.0$	$\mu\text{mol/ml.h}$
Navozym 435	$106 \pm 2.5$	$\mu\text{mol/g.h}$
L-ZIF	$123.5 \pm 2.5$	$\mu\text{mol/g.h}$
ZIF-8	21.0	$\mu\text{mol/g.h}$

The comparison of the enzyme solution used in preparing it, commercial immobilized lipase, Novozyme 435, and the ZIF without enzyme are shown in Table 4, in which one unit enzyme activity is defined as amount of the enzyme that produces 1  $\mu\text{mol}$  of fatty acids per hour as equation 17. As shown in Table 4, the activity of Eversa Transform 2.0 solution, which was measured 5 times, was 236  $\mu\text{mol/ml.h}$ . As

1 ml of diluted enzyme solution was used in the preparation of the encapsulated L-ZIF, the activity provided in the preparation solution was 236 U. The amount of produced L-ZIF was  $0.4 \pm 0.05$  g, with an activity measured to be 210 U per 1 g. Therefore, the activity of produced 0.4 g L-ZIF is 84 U. The activity of the empty ZIF-8 was measured to be 21 U/g, and hence the activity of the 0.4 g empty ZIF-8 is 8.4. After deducting the activity of the empty ZIF-8 from that of the L-ZIF, the fraction of the provided enzyme that was encapsulated inside the L-ZIF was calculated to be 32.0%. However, it should be noted that besides incomplete encapsulation of the enzyme, the drop in the activity could also be due to mass transfer limitation encountered with the immobilized enzyme in the ZIF-8. The encapsulation of lipase inside ZIF-8 was comparable to that of catalase in ZIF-8, which was 42.3% of the activity of the enzyme used in the preparation (Du et al., 2017).

In addition, the activity Novozyme435, which is a commercially available *Candida antarctica* lipase immobilized on a resin commonly used in biodiesel production (Moreira et al., 2020), was also measured. The comparison is shown in Table 4, in which one unit enzyme activity is defined as the amount of the enzyme that produces 1  $\mu\text{mol}$  of fatty acids per hour. By replacing the catalase with nanobiocatalyst, a much higher encapsulation percentage of 87.4% was achieved (Du et al., 2017). The Nanobiocatalyst (NBC) is a modern bioprocessing technique that blends advanced nanotechnology with biotechnology to offer exciting benefits (Mission, Zhang & Jin, 2015). The L-ZIF was prepared by the first method will be described in Chapter 4.5, and the results we obtained by repeating twice. Pitzalis (2018) studied encapsulated of *Pseudomonas fluorescens* (lipase AK) and *Rhizomucor Miehei* (RM) in the ZIF-8 and the activity of AK@ZIF-8 and RM@ZIF-8  $84.5 \pm 0.3$  U  $\text{mg}^{-1}$  and  $75.8 \pm 0.4$  U  $\text{mg}^{-1}$ , respectively (Pitzalis et al., 2018).

### 3.2 Immobilization Capacity

Protein content was used to determine the immobilization capacity and to have a consistent basis for results comparisons, which would allow mass transfer determination. The protein concentration in a sample was measured by adding a Bradford reagent and measuring the optical absorption at 595 nm using a spectrophotometer (Spectrostar Nano, Germany). The concentration was then determined using a calibration curve of serial dilutions of known protein concentration.

To determine the adsorption capacity of the ZIF-8, 1.27 mg of already prepared empty ZIF-8 was soaked in 10 ml of lipase solution (5 times dilution) for 6 h under continuous stirring using magnetic stirrer. The protein concentration at time zero and at the end of the experiment, after the ZIF was separated by centrifugation, following by vacuum filtration were measured. The background used in the spectrophotometry was distilled water. The adsorption lipase on ZIF-8 was determined to be  $4.67 \pm 0.54$  mg-protein/g-ZIF from the difference of the two protein concentrations multiplied by the sample volume and dividing by the amount of ZIF-8 used.

To determine the encapsulated protein in ZIF-8, the proteins concentration before encapsulation and in the supernatant after the removal of the produced crystals were measured. In this case, the background was the initial solution used to prepare the empty ZIF, consisting of 5 ml of zinc acetate, 20 ml of 2-merthylimidazole and 10 ml of distilled water (instead of 10 ml of the enzyme solution used in the preparation of the encapsulated lipase). The encapsulated lipase in ZIF-8 was determined to be  $9.07 \pm 0.01$  mg-protein/g-ZIF from the difference of the two protein concentrations multiplied by the sample volume and dividing by the amount of ZIF-8 used. There are several studies to measure the amount of proteins, one of them was it is the

immobilized of Glucose Oxidase GX inside ZIF-8 which is an enzyme have been used to remove glucose acid. The amount of proteins used in ZIF-8@Cellu@Fe<sub>3</sub>O<sub>4</sub> was 94.26 mg/g (Cao et al., 2016), and This high value because they enhance their encapsulated by used magnetic regenerated cellulose-coated nanoparticle. Previous studies have focused on MOF-functionalized magnetic nanoparticles that can be recycled under magnetic field and have excellent physical and chemical MOF characteristics in order to effectively distinguish MOF-based materials (Cao et al., 2017).

### **3.3 Crystal Structure**

The effect of encapsulating the enzyme on the crystal structure of the ZIF-8 was determined using the XRD measurements of the empty ZIF-8 and encapsulated L-ZIF. The L-ZIF was prepared as described in Section 2.2.

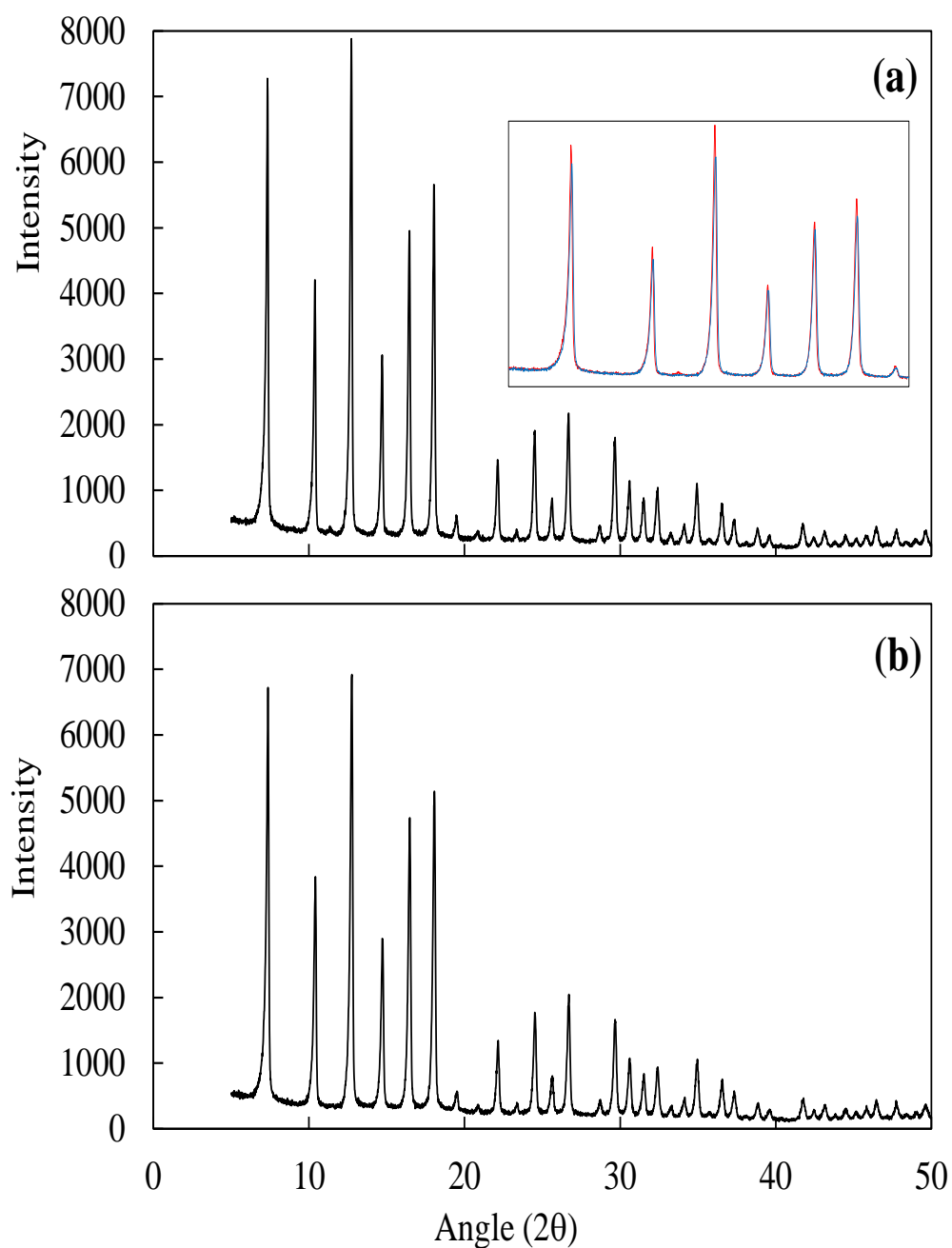


Figure 7: XRD of empty ZIF-8 and L-ZIF, (a) empty ZIF-8 and (b) L-ZIF

As shown in Figure 7, the topology of the ZIF-8 and encapsulated L-ZIF have approximately similar spectrums, which indicate that enzyme immobilization did not affect the crystals of the ZIF-8. However, the peaks of ZIF-8 were slightly higher than those of encapsulated L-ZIF, which suggests that it has more defined structure. Similar

results to those found in this work were obtained by comparing the XRD pattern of ZIF-8 to those of lipases, from *Rhizomucor Miehei* encapsulated in ZIF-8 (Adnan, Li, Xu, & Yan, 2018). Similar results were also observed with other enzymes, such as catalase, encapsulated inside ZIF-8 (Du et al., 2017). However, slightly higher, rather than lower, peaks were observed when lipase from *Burkholderia Cepacia* was encapsulated in ZIF-8 (Adnan, Li, Wang, Xu, & Yan, 2018), which could be attributed to the differences in the preparing methods.

### **3.4 Morphology Analysis**

To examine the effect of the enzyme encapsulation on the ZIF-8 morphology, Scanning Electron Microscope (SEM) was used to compare the shape of the crystals of ZIF-8 with and without enzyme encapsulation as described in Section 2.2, and the results are shown in Figure 8. Figure 8 shows that both encapsulated L-ZIF and empty ZIF-8 have clear hexagonal prism shapes, which agrees with previous studies done on ZIF-8 (Begum, Hussain, & Noor, 2020; N.-L. Liu et al., 2016; Nadar & Rathod, 2018). Similar results to those found in this work were observed by comparing the morphology of ZIF-8 to that of lipase encapsulated in ZIF-8 (Nadar & Rathod, 2018) and in ZIF-67 (Rafiei et al., 2018). It was observed that, although the presence of the enzyme in the solution during crystallization did not affect the shape of the produced crystals, a slight drop in the size of the crystals was observed. A more significant drop in size was observed in work of Adnan and his team when lipase was encapsulated in ZIF-8 (Adnan, Li, Xu, & Yan, 2018; Song et al., 2012). This suggests that the protein within the crystals may have affected the growth of the crystals. However, another hierarchical shape of ZIF-8 was observed, when the ZIF was prepared with different variable Hmim / Zn ratios and difference of Zn salts besides to as the amount of Hmim



increased will produce the smaller particles size (Adnan, Li, Xu, & Yan, 2018; Adnan, Li, Wang, Xu, & Yan, 2018; Jian et al., 2015).

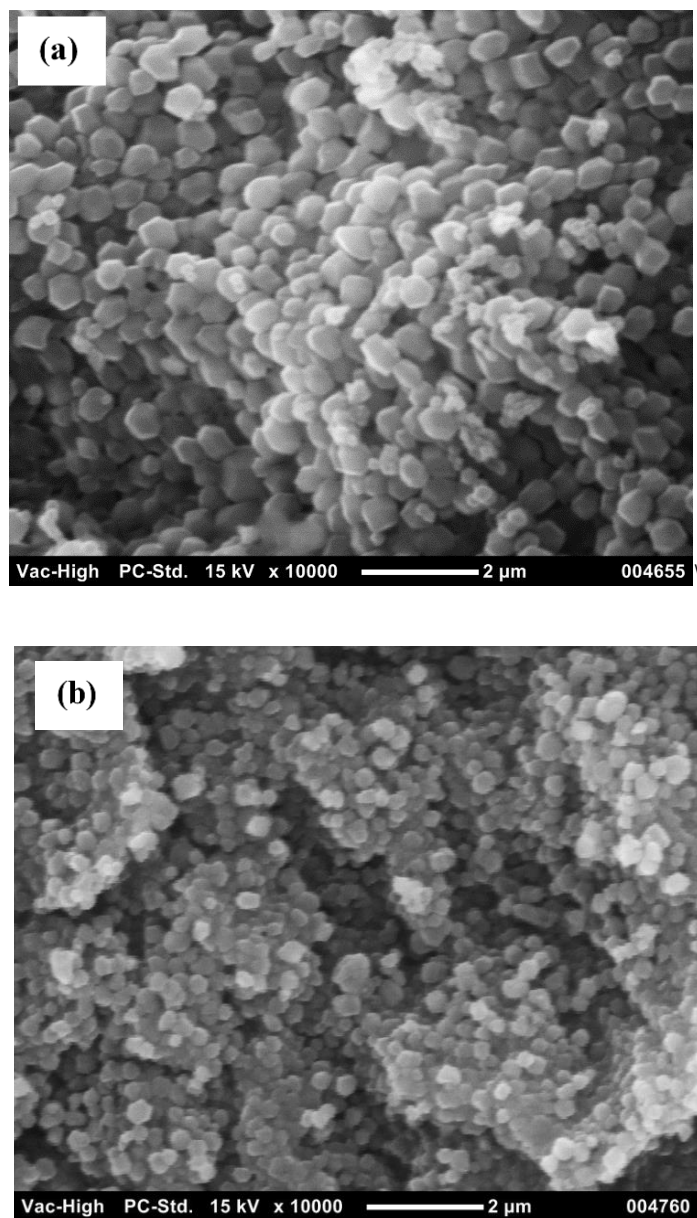


Figure 8: Scanning Electron Microscopic (SEM) images of empty ZIF-8 and L-ZIF

### 3.5 Pore Size Analysis

$N_2$  Adsorption isotherms at 77 K of the prepared empty ZIF-8 and the ZIF-8 with encapsulated lipase are shown in Figure 9. Both samples showed a type-I (IUPAC classification) isotherm of a sharp uptake at low relative pressures, which is a typical feature of microporous materials. The isotherm also suggests that the pores have homogeneous distribution in the micropores range. The Brunauer–Emmett–Teller (BET) surface area of pure ZIF-8 was measured to 949.7  $m^2/g$ . After encapsulation with lipase, the BET surface area dropped to 666.3  $m^2/g$ , which corresponds to 29.8% drop. The mean pore size also dropped by lipase encapsulation from 0.551 nm for empty ZIF to 0.386 nm for L-ZIF. The drop in the BET surface area and pore sizes is an indication of the lipase molecules filling the pores of the ZIF-8. The BET surface area of the ZIF-8 found in this work was lower than that of the macroporous ZIF-8 prepared in our previous work, which was 1636  $m^2/g$  (Hu, Dai, Liu, & Du, 2020). Nevertheless, with lipase immobilization, the BET surface area was also found to drop, by 22%, to 1276  $m^2/g$ . The lower percentage drop reported in our previous work was mainly because the lipase was immobilized by adsorption, whereas in this work, the immobilization was by encapsulation, which is expected to fill the internal pores.

The average surface area of the ZIF-8 was also reported in literature to be between 1300–1600  $m^2/g$  (Song et al., 2012). The Pore radius size of ZIF-8 0.551  $cc/g$ , while the pore radius of L-ZIF is 0.384  $cc/g$ . The pore size of the synthesized ZIF-8 nanoparticles was found to be 60 nm and directly integrated into the polymer matrix model. (Song et al., 2012). Liu and his team reported hierarchically porous immobilization of bacillus subtilis lipase and the average mesopore size is around 34 nm (Y. Liu et al., 2011). while the pore size of ANG@M-ZIF-8(*Asperigullus niger*

lipase), which the complex diffusion synthesized into the macropores, is about 200 nm (Hu et al., 2020).

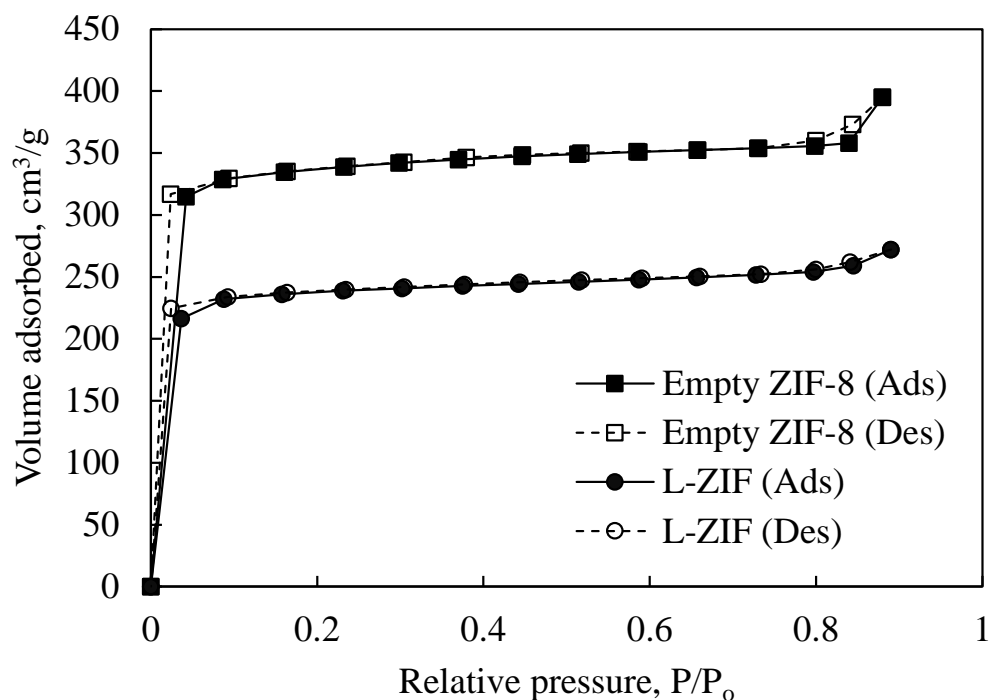


Figure 9: N<sub>2</sub> adsorption isotherms of ZIF-8 empty and encapsulated lipase at 77 K

### 3.6 Fourier Transform Infrared (FT-IR)

The chemical structure of pure ZIF-8 and L-ZIF by using FT-IR are shown in Figure 10. (Rafiei et al., 2018). The wavenumber range was 599 to 4000 cm<sup>-1</sup> correspond to the imidazole ring's typical stretching and bending modes. C–N bending vibration and C–H bending mode, respectively, may be attributed to the maxima at 995 and 760 cm<sup>-1</sup>. The signals between 1300 and 1460 cm<sup>-1</sup> were for the whole ring

stretching, whereas the band at 1146 cm<sup>-1</sup> was for aromatic C–N stretching mode (Garmroodi et al., 2016).

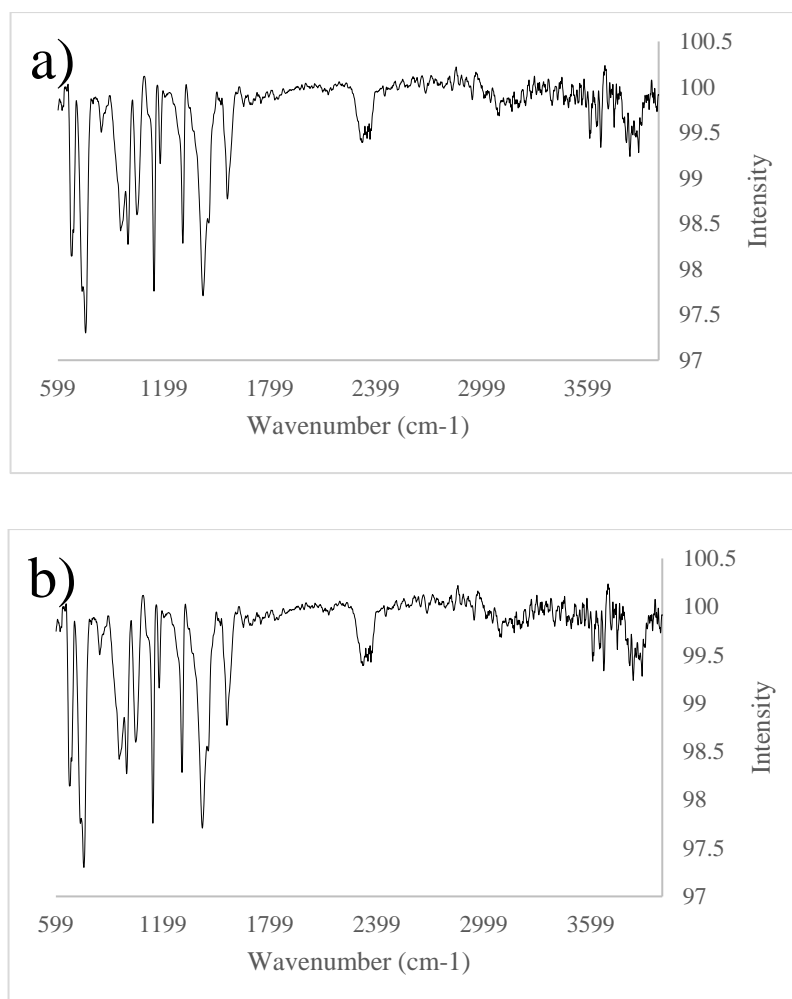


Figure 10: FT-IR spectra of pure ZIF-8 (without lipase, ZIF-8) and FT-IR spectra L-ZIF. (a) ZIF-8 (b) L-ZIF.

### 3.7 Different Production Technique of Biodiesel Production

The analysis of the chemical composition of the olive oil was performed by Gas Chromatography (GC). The results with the free fatty acids present in the residual oil are shown in the chromatogram presented in Figure 14.

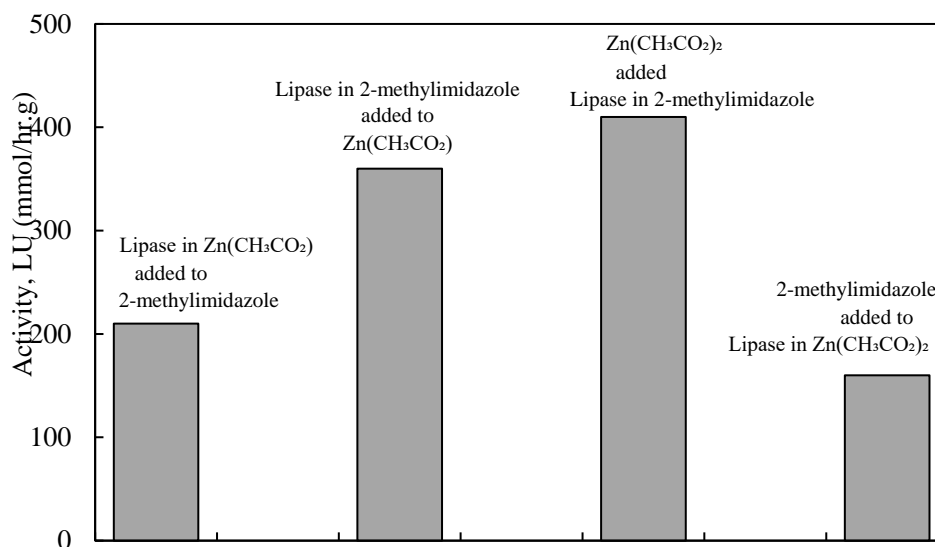


Figure 11: Effect of L-ZIF preparation on the activity (without dilution of enzyme)

The Figure 11 shows effect of L-ZIF preparation on the activity and the preparation methods was similar to the section 2.3 except the difference in the dilution factor of the enzyme. In the section 3.1, the result was based on 10 times diluted of the lipase, whereas here the experiment was done without any dilution.

### 3.8 Biodiesel Production

#### 3.8.1 Enzyme Immobilization

To further confirm the encapsulation of the lipase inside the ZIF, encapsulated L-ZIF, was used to produce biodiesel from olive oil, and compared to empty ZIF-8 and with no enzyme, as shown in Figure 12.

The results clearly show that after 4 h of reaction, almost no biodiesel was produced when no enzyme and empty ZIF-8 were used. However, when encapsulated

L-ZIF was used, the production rate significantly increased. The presented results are the average of four repetitions. The standard deviations were shown as error bars, which confirm the reproducibility of the results. For better comparison, the yield using the soluble enzyme, shown in Figure 12, was normalized to the same activity of the used L-ZIF. It is clearly seen that the soluble enzyme resulted in a higher yield, which is mainly due to the diffusion resistance encountered with the immobilized enzyme.

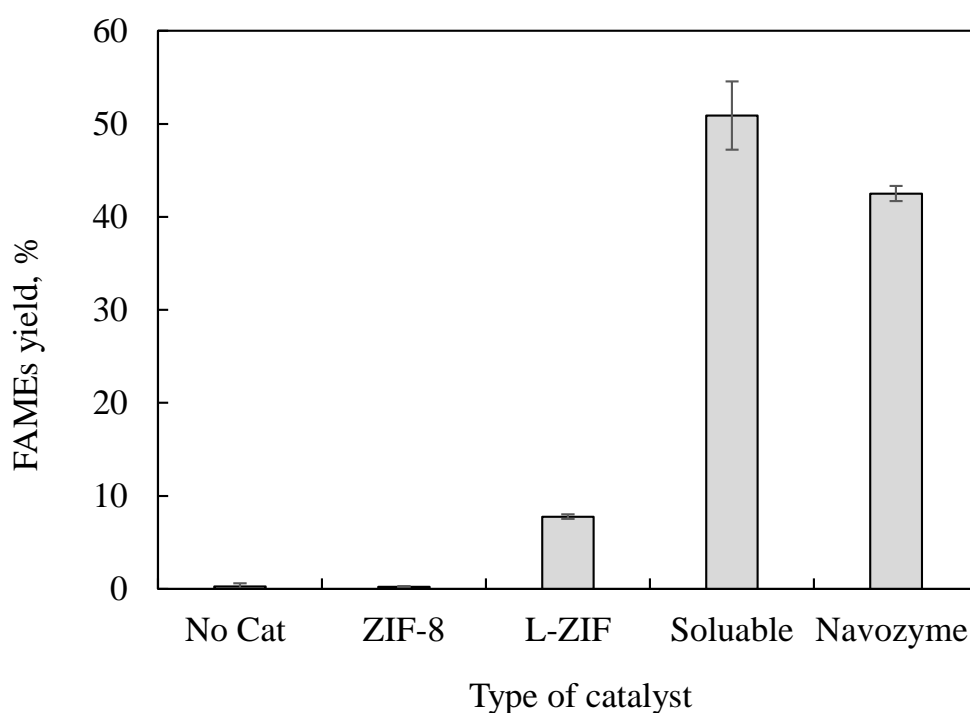


Figure 12: Biodiesel yield after 4 h using L-ZIF as compared to soluble enzyme, Novozym435, empty ZIF-8 and no catalyst, at 1:12 M:O ratio and 40°C (with immobilized enzyme 0.2 g and with soluble enzyme 0.5 ml were used)

### 3.8.2 Encapsulated vs Adsorbed L-ZIF

The surface adsorption capacity of ZIF-8 towards lipase was determined from the amount of attached proteins in previously prepared and activated empty ZIF-8 and

was compared to the capacity of ZIF-8 by encapsulation of the enzyme during the crystals' formation, as described in Section 2.10. It was found that larger enzyme loading was achieved by lipase encapsulation, which was  $9.07 \pm 0.01$  mg-protein/g-ZIF, compared  $4.67 \pm 0.54$  mg-protein/g-ZIF achieved by adsorption. This is mainly due to the difficulty of lipase to penetrate deeper into the micropores of the empty ZIF-8 and utilize the entire available pores. However, when the two immobilized enzymes (adsorption and encapsulation) were used for the production of biodiesel from olive oil, the yield using the adsorbed lipase was higher than that of the encapsulated one, at both methanol concentrations tested, as shown in Figure 13.

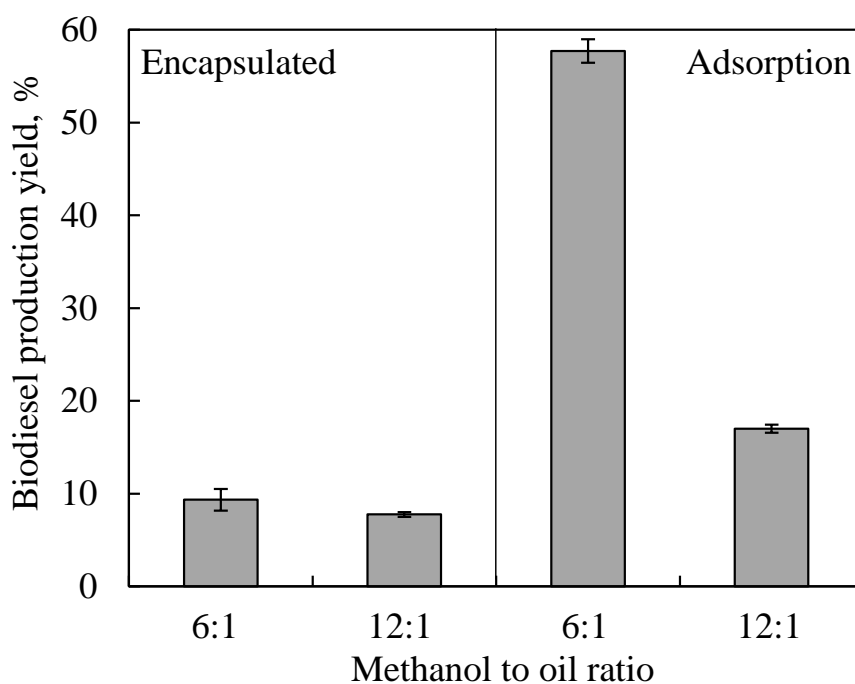


Figure 13: Effect of methanol to oil ratio on the biodiesel production yield, after 4 h of reaction using 0.5 g oil, 0.2 g L-ZIF (encapsulated and adsorbed)

This further confirms the mass transfer limitation effect, which is much higher in the encapsulated enzyme. In both cases, increasing the methanol concentration

resulted in a drop in the yield, owing to the methanol inhibition effect Production of Biodiesel: Possibilities (Sulaiman, 2007). The drop in the yield could also be attributed to the dilution effect with the increase in added methanol amount. However, owing to the low molecular weight of methanol, as compared to the oil, the amount of methanol added to bring its ratio to 6:1 or 12:1 was small, and the change in the overall reaction volume dropped from 2.65 ml for the case of 12:1 methanol to oil ratio 2.40 ml for the case of 6:1, rendering the latter dilution effect less significant than that of methanol inhibition.

As mentioned earlier, for the enzymatic process to be economically feasible, repeated reuse of the enzyme is essential (Rafiei et al., 2018). Despite the higher activity of the adsorbed lipase on ZIF-8, as shown in Figure 13, the adsorption forces are relatively weak, and hence the adsorbed lipase on post-synthesized ZIF-8 is prone to leaching. Hence, it is expected to have a lower usability as compared to encapsulated lipase inside ZIF-8. To verify that, the reusability of lipase immobilized on ZIF-8 by adsorption and encapsulation was investigated in the transesterification of olive oil with methanol. Experiment similar to the one described in Section 2.5 was carried out, but in this case, after removing the product, the immobilized lipase was separated by centrifugation (4500 rpm, 5 min), washed with n-hexane, and reused with fresh oil and methanol. The experiment was repeated for 5 runs, and the results are shown in Figure 14.

The Percentage recovered activity of each cycle, shown in Figure. 17, were based on the initial activity in the first cycle. The results clearly show a higher stability of the encapsulated lipase compared to the adsorbed one. At methanol ratio of 12:1, the encapsulated lipase in ZIF-8 maintained 83% residual activity in the fifth cycles,



as compared to the activity in first cycle. Whereas, at the same methanol ratio, adsorbed lipase on ZIF-8 maintained only 34% residual activity. Similar superiority of the encapsulated lipase in ZIF-8 over the adsorbed one was also observed at methanol ratio of 6:1, wherein the encapsulated lipase maintained 64% residual activity, compared to only 10% for the adsorbed. The initial drop-in activity is expected to be because of the loss of weakly attached enzyme, leaving behind only the encapsulated enzyme inside the pores that are preserved and not lost from one cycle to the next. However, with the post synthesis adsorption case, the enzyme kept leaching in every cycle, resulting in continuous drop in the activity. This suggests that despite the higher activity of adsorbed lipase on ZIF-8, the instability with repeated reuses could make encapsulated lipase more favorable.

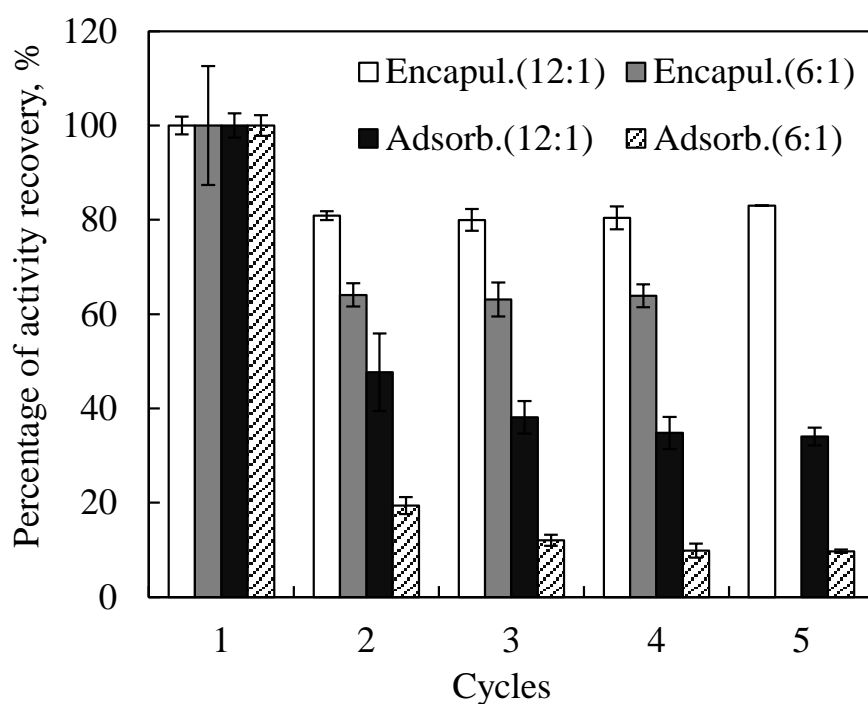


Figure 14: Percentage recovered activity based on the first cycle, after several biodiesel production cycles at methanol ratios of 12:1 and 6:1. Each cycle was for 4 h using 0.5 g oil, 0.2 g L-ZIF (encapsulated and adsorbed)

Despite the higher initial activity at 6:1 methanol:oil ration, it was found that the residual activity at 12:1 was higher, for both immobilization techniques. It should be noted that in the case of adsorbed lipase, the absolute residual activity at 6:1 was still higher than that of 12:1. However, as the initial activity at 6:1 was significantly higher, the residual activity ratio relative to the initial activity was lower. The reason for the higher drop at 6:1 methanol ratio, as compared to 12:1, was mainly due to the larger glycerol production in the first cycle, which was not removed using the protocol adopted in this work. To remove the by-product glycerol, the recovered enzyme is usually washed with tert-butanol, as used by Rafiei and her team (Rafiei et al., 2018) with lipase encapsulated in ZIF-67, and in our previous work (Sulaiman, 2007) using Novozyme in an ionic liquid. Nevertheless, even without the removal of glycerol, a

similar residual activity of 64% in the fourth cycle was achieved in this work at methanol molar ratio of 6:1, as compared to that obtained by Rafiei and her team (Rafiei et al., 2018), which was 65%, at the same methanol ratio, even when methanol was added in 3 steps to minimize the inhibition effect. Although, the stepwise addition of methanol and the removal of glycerol did not show a significant effect on enhancing the stability, the yield obtained by Rafiei and her team (Rafiei et al., 2018) reached 80% after 60 h of reaction.

### **3.8.3 Biodiesel Production Rate**

This experiment was conducted to determine the time progress of olive oil conversion using encapsulated L-ZIF. The results shown in Figure 15 are the average values of 4 repetitions, and the reproducibility of the results were determined from the standard deviations presented as error bars in the Figure 15.

As time increased, the FAME yield increased and the oil concentration dropped almost linearly reaching a value of 56 mg/ml after 24 h, corresponding to 44% conversion yield. This yield was lower than that found for soybean oil using 92.3 w/w% RML encapsulated in X-shaped ZIF-8, at 1:4 oil:ethanol ratio and 30°C, which was 92% after 24 h (Adnan, Li, Xu, & Yan, 2018). However, the specific activity of the enzyme used was not reported in this work. In addition, the reaction was carried out in isooctane medium, which was reported to have a positive effect of reacting with residual amino acids in the lid of the enzyme, resulting in increasing its activity.

A better result was also obtained for soybean oil using BCL-ZIF-8 at oil to ethanol 1:4 ratio and 40°C, which was 91.7% after 12 h (Adnan, Li, Wang, Xu, & Yan, 2018). The main reason for those differences is the activity of the enzyme used. In the

work of RML@ZIF-8 the highest activity was 2632% at 20 hr at 25 mg of lipase. However, with BCL@ZIF-8 the highest activity recovery was 1103% at 30 min by used 700 mg of lipase. The BCL enzyme activity attained was 50200 U/g (Ke, Li, Huang, Xu, & Yan, 2014), and the activity of RML was 20000 U/g lipase (Garmroodi et al., 2016).

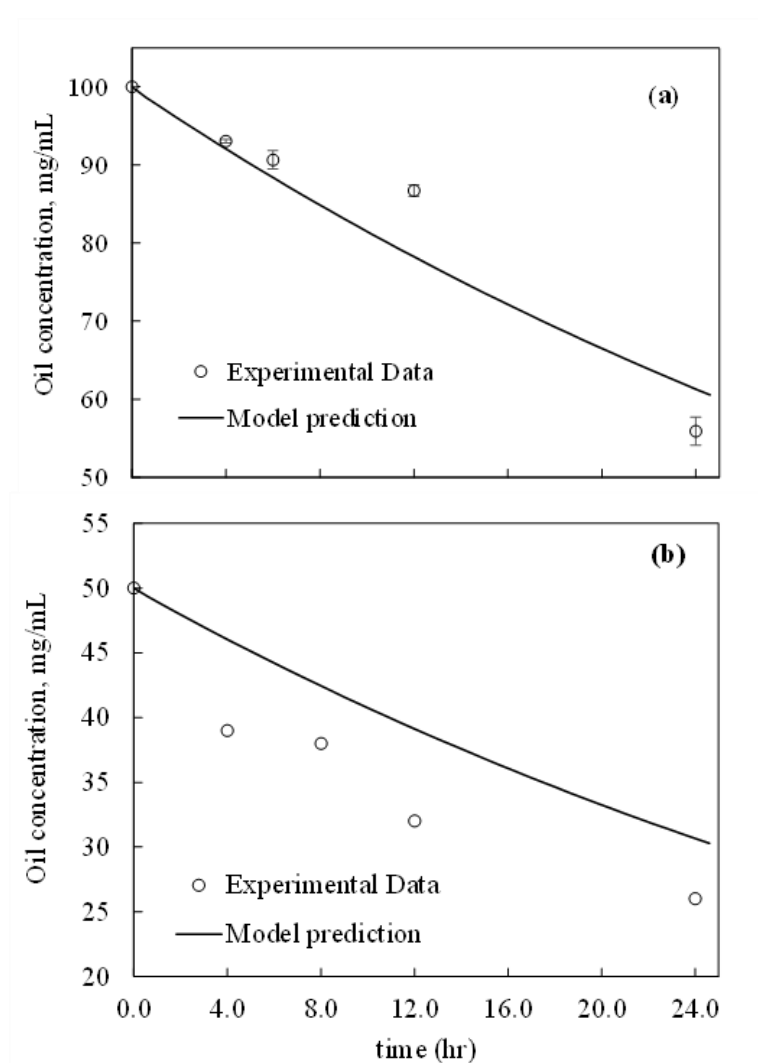


Figure 15: Comparison between the experimental and model prediction of the drop in oil concentration, using 20% per oil encapsulated L-ZIF at 40°C and methanol to oil of 12:1 using concentration of 100 mg/mL and 50 mg/mL. (a) 100 mg/ml and (b) 50 mg/ml

The activity of soluble lipase (Eversa) was 123.5 U/g, which was lower compared to their enzyme activity. This highest activity at the high concentration of enzyme loading could lead to an adsorption multilayer on the hydrophobic structure, decreasing the porous diameter and limiting diffuse growth. Besides that, in BCL, the highest activity was done by used adsorbent encapsulated.

#### **3.8.3.1 Effect of Substrate Amount**

The effect of substrate amount on the initial rate of reaction using encapsulated L-ZIF is shown in Figure 16.

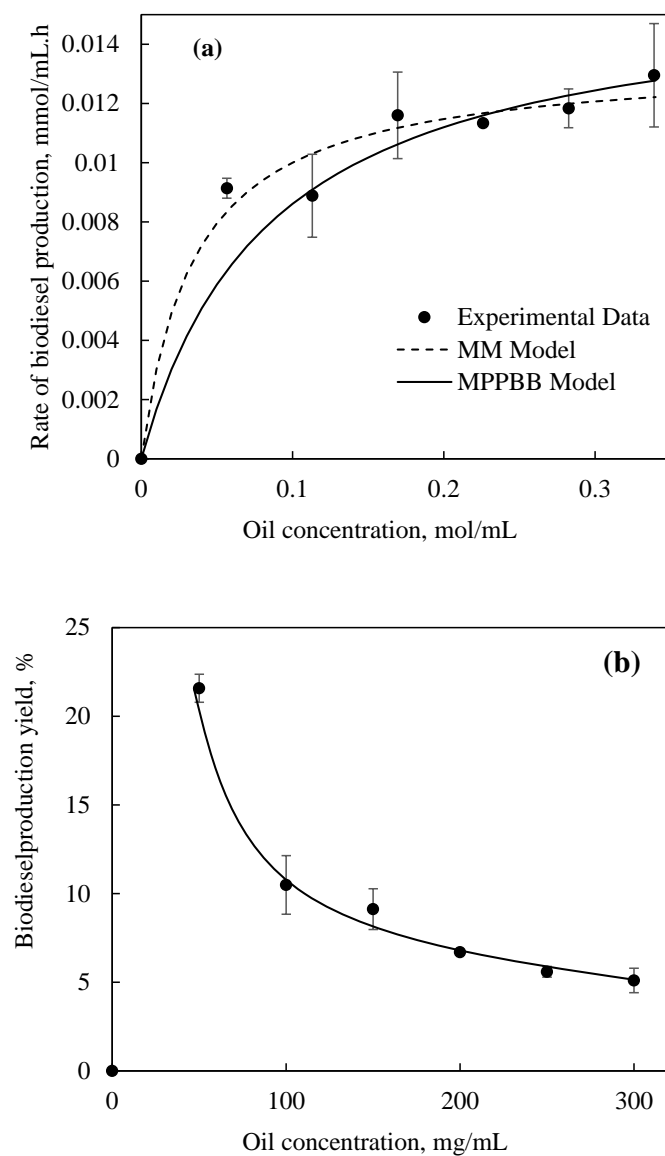


Figure 16: Effect of oil concentration on initial rate of biodiesel production and production yield, after 4 h reaction using 12:1 methanol:oil ratio, 40°C and 0.2 g encapsulated L-ZIF.

As shown in Figure 16, the change of the produced amount of FAME with time in the first 4 h of reaction was linear. Therefore, the initial rate of reaction at different initial substrate concentration was determined by dividing the determined amount of FAMES, produced in 4 h, by 4. The results are average values of duplicate repetitions, and the reproducibility of the results were determined from the standard deviations

presented as error bars. In this experiment, the amount of methanol was changed, to maintain a constant molar ratio at 12:1, and the added n-hexane amount was adjusted to keep the overall reaction volume constant at 10 ml. It can be seen that the reaction rate increases with increasing the substrate concentration, and then it reaches a plateau, which suggests that the reaction can be presented by the Michaelis Menten (MM) kinetics, given in Equation (19).

$$v = \frac{V_{\max}[S]}{K_S + [S]} \quad (19)$$

Where,  $v$  and  $V_{\max}$  are the initial rate and the maximum rates of reaction, respectively, and  $K_S$  is dissociation constant of the substrate,  $[S]$ . The experimental data, shown in Figure 16-a, were used to fit the MM model using Excel solver to adjust the kinetics parameters by minimizing the objective function given in Equation (20).

$$\text{O.F.} = \sum (v_{\text{pred}} - v_{\text{exp}})^2 \quad (20)$$

Where,  $v_{\text{pred}}$  and  $v_{\text{exp}}$  are the experimental and predicted initial rate of reaction, respectively.

Al-Zuhair developed a more comprehensive mathematical model from the kinetic mechanistic steps of the reaction, which considers the inhibition by both substrates (Sulaiman, 2007). The developed Modified Ping Pong Bi Bi (MPPBB) model is given in Equation (21). Excel solver was also used to determine the kinetics parameters by minimizing the objective function in Equation (20)

$$v = \frac{V_{\max}}{1 + \left(\frac{K_{iA}}{[A]}\right) \left[1 + \left(\frac{[S]}{K_S}\right)\right] + \left(\frac{K_{iS}}{[S]}\right) \left[1 + \left(\frac{[A]}{K_A}\right)\right]} \quad (21)$$

Where,  $K_S$  and  $K_{iS}$  are the dissociation and inhibition constants of the substrate,  $[S]$ , respectively, and  $K_A$  and  $K_{iA}$  are the dissociation and inhibition constants of the

alcohol, [A] and, respectively. Figure 16-a shows comparison between the experimental data and model predictions using the determined model parameters given in Table 5. As shown in the figure 16-b, since substrate and alcohol inhibitions were not encountered within the tested range, MM model was adequate in presenting the experimental data. Nevertheless, the MPPBB model developed by Al-Zuhair and his team. (Sulaiman, 2007) still showed a better prediction with  $R^2$  value closer to 1.0.

Table 5: Kinetics model parameters of biodiesel production catalyzed by encapsulated lipase in ZIF-8

Model parameter	Encapsulated Lipase in ZIF-8		Free Lipase	
	MM Model	MPPBB Model	MM Model	MPPBB Model
$V_{\max}$ ( $\text{h}^{-1}$ )	0.013457	0.319426	0.330582	1.491522
$K_S$ (mol/ml)	0.03456	1.640166	0.491428	1.145605
$K_A$ (mol/ml)	-	0.891706	-	1.806186
$K_{iS}$ (mol/ml)	-	1.0425	-	2.114428
$K_{iA}$ (mol/ml)	-	1.016075	-	1.004119
$R^2$	0.969	0.989	0.916	0.966

The effect of substrate amount on the biodiesel production yield from olive oil after 4 h, using encapsulated L-ZIF is shown in Figure 16-b. Despite the increase in reaction rate with the increase in oil concentration, as shown in Figure 16-a, the substrate concentration effect showed an opposite effect on the total biodiesel production yield after 4 h. This drop should not be misinterpreted as substrate inhibition, which was clearly not encountered, as shown in Figure 17-a. The drop observed in Figure 17-b was rather because the increase in the produced biodiesel was not linear and increased in an order less than that of the increase in the oil concentration. Hence, dividing the amount produced by the initial amount of oil used



resulted in this observed decrease in the yield, and the maximum yield of 22% was observed at the minimum substrate concentration of 50 mg/ml.

The effect of substrate amount on the initial rate of reaction using free lipase was also tested, and the results are shown in Figure 17-a. The results are average values of duplicate repetitions, and the reproducibility of the results were determined from the standard deviations presented as error bars. The experimental data were used to fit the MM and MPPBB models using Excel solver.

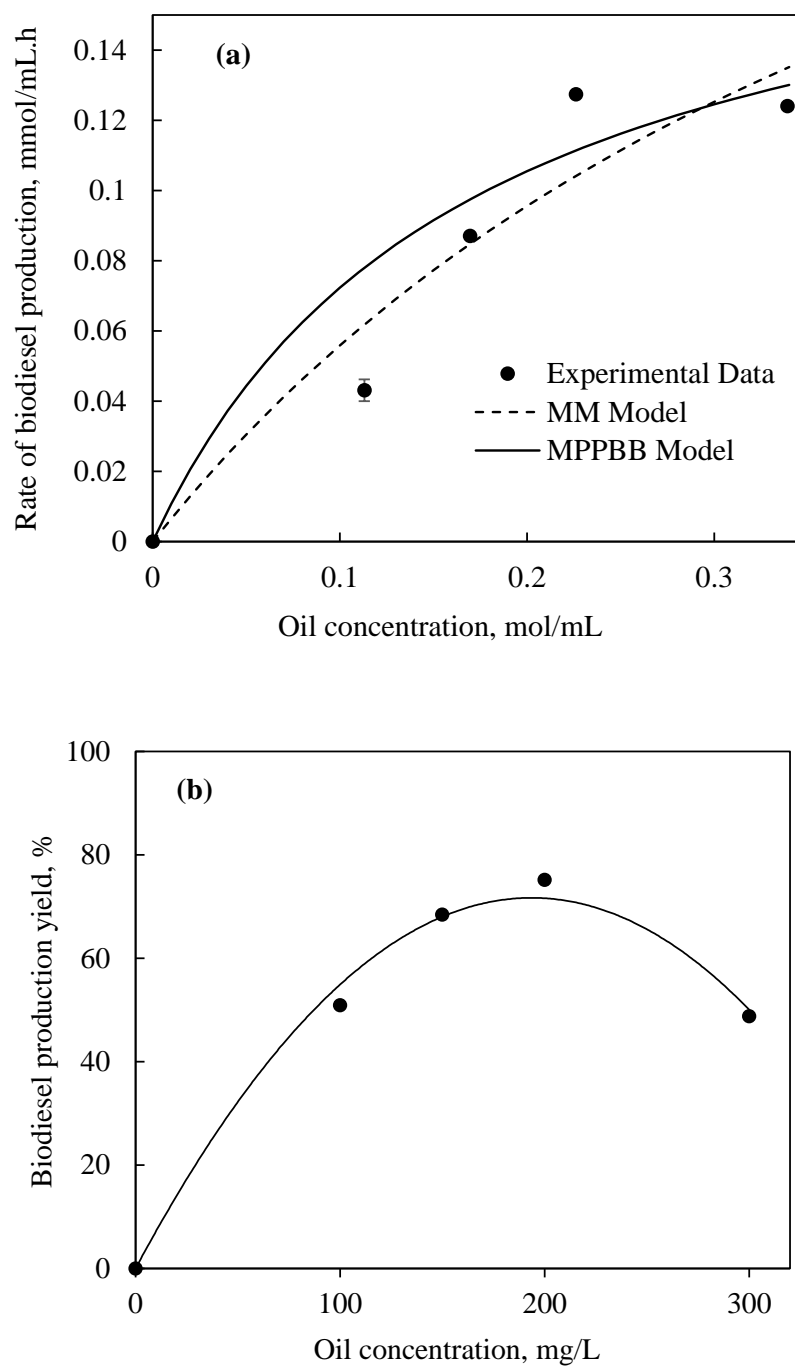


Figure 17: Effect of biodiesel production and production yield of oil concentration on initial rate, after 4 h reaction using 12:1 methanol:oil ratio, 40°C and 0.5 ml soluble enzyme

Figure 17-a shows comparison between the experimental data and the model predictions using the determined model parameters given in Table 5. Similar to the

case of the immobilized lipase, MM model was adequate to present the experimental data. Nevertheless, the MPPBB model still showed a better prediction with  $R^2$  value closer to 1.0. The effect of substrate amount on the biodiesel production yield from olive oil after 4 h, using free lipase is shown in Figure 17-b. With the free enzyme, the yield increases initially up to substrate concentration of 200 mg/ml at which the maximum yield of 75% was achieved, and then the yield dropped.

### **3.8.3.2 Effect of Methanol Ratio and Temperature**

The effects of methanol amount and temperature on the yield of biodiesel production from olive oil after 4 h, using encapsulated L-ZIF are shown in Figure 18. The presented results are the average values of triplicate repetitions, and the reproducibility is determined from the standard deviations shown as error bars. It can be seen that increasing the methanol ratio resulted in decreasing the reaction yield. This was due to negative effect of the short carbon chain alcohol on the activity of the enzyme, what is known as alcohol inhibition (Hu, Dai, Liu, & Du, 2020). A similar optimum methanol ratio of 1:6 was also observed using lipase encapsulated in ZIF-67 tested on biodiesel production from soybean oil Soybean oil at 45°C (Rafiei et al., 2018). As mentioned in Section 3.8.2., the drop in the yield was attributed to the dilution effect by the increase in methanol amount.

Figure 18 also shows that increasing the temperature from 40 to 50°C, resulted in a significant drop in the production yield. This is mainly due to the denaturation of the protein at the higher temperature, which in turn reduced the enzyme activity. This result agrees with that found with soybean oil transesterification, which shows an optimum temperature at 45°C (Adnan, Li, Xu, & Yan, 2018). A similar finding was

also reported using encapsulated lipase in ZIF-67 in which the activity significantly dropped at temperatures above 45°C (Rafiei et al., 2018).

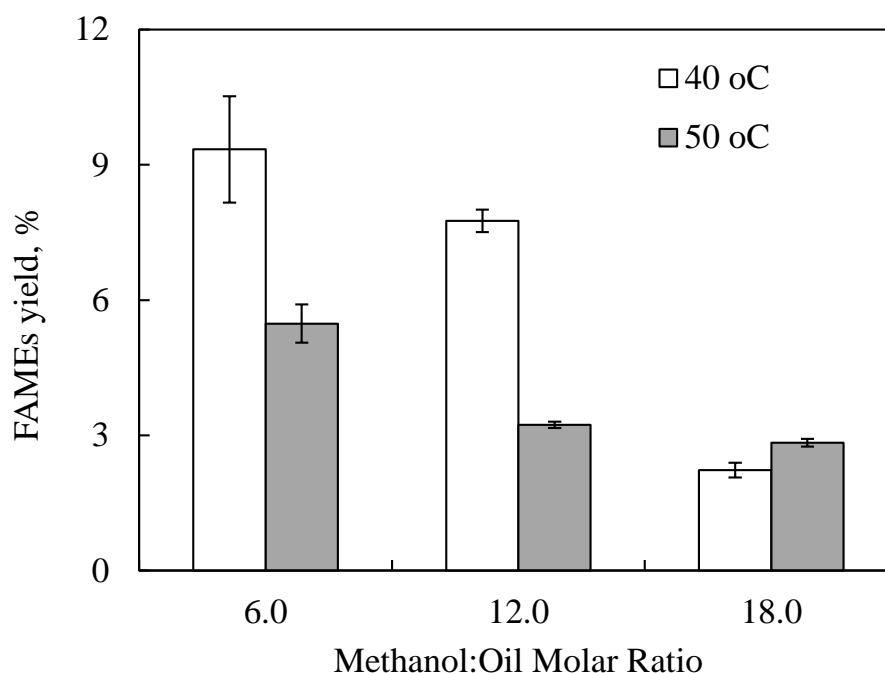


Figure 18: Effect of temperatures and methanol to oil molar ratio, on FAEEs production after 4 h, using 20% L-ZIF

### 3.8.3.3 Effect of Water Content in Biodiesel Production

The effect of water content on biodiesel production yield from olive oil after 4 h, using L-ZIF prepared by adding  $\text{Zn}(\text{CH}_3\text{CO}_2)_2$  to lipase in 2-methylimidazole was tested. The results shown in Figure 19. To determine the effect of water on the biodiesel production yield, the experiment was repeated using 12:1 methanol ratio and encapsulated Lipase in ZIF and different amounts of water. The biodiesel production yield after 4 of reaction was determined. It can be seen that the yield decreased with the increase in initial water content. This drop is mainly because excess water stimulates the competing hydrolysis reaction (Sulaiman, 2007). A similar drop in

methanolysis was observed using Novozym@435, which was inhibited at a water content of only 0.1% water.

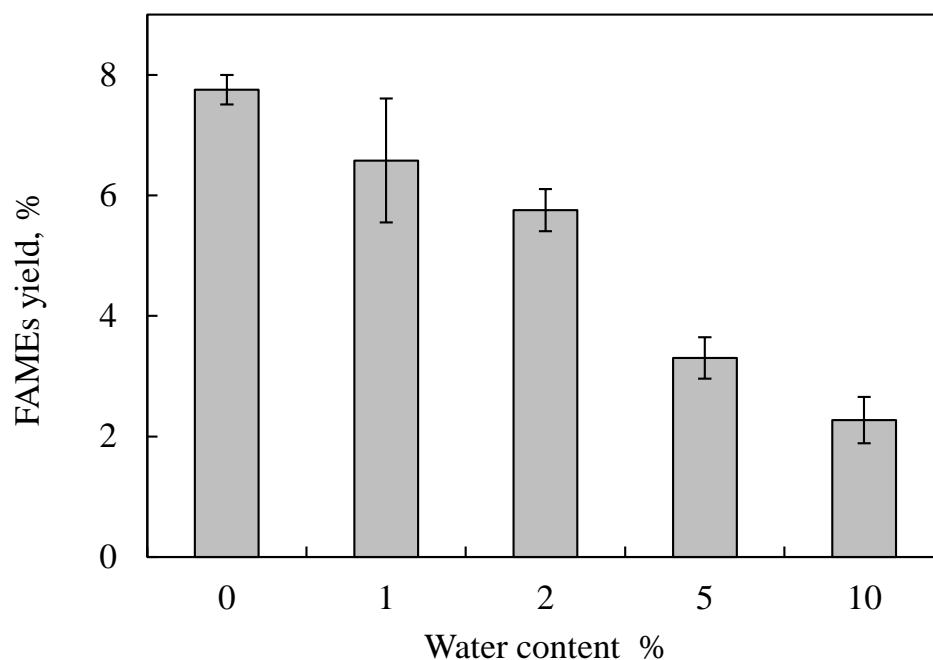


Figure 19: Effect of the water content on FAEs production, after 4 h using 20% L-ZIF at 40°C and 12:1 M:O ratio

### 3.9 Diffusion-Reaction Model

Equations (13-16) were solved simultaneously using Excel spreadsheet, using the diameter of the prepared ZIF-8 of 0.18  $\mu\text{m}$ , as determined by the SEM, ZIF-8 density of 960  $\text{mg cm}^{-3}$ , reaction volume of 10  $\text{cm}^3$ , mass of ZIF-8 used of 200 mg and the  $V_{\text{max}}$  determined by the Michaelis Menten model of 0.013  $\text{h}^{-1}$ , as described in Section 3.8.3. The value of  $D_s$  was then changed to obtain the best fitting of the results.

$$S_{r,i}^{n+1} = S_{r,i+1}^n \Delta t \left( \frac{D_s}{\Delta r^2} + \frac{2D_s}{r\Delta r} \right) + D_s \Delta t \frac{S_{r,i-1}^n}{\Delta r^2} - S_{r,i}^n \left[ \Delta t \left( \frac{2D_s}{\Delta r^2} + \frac{2D_s}{r\Delta r} + V_{\text{max}} \right) + 1 \right] \quad (13)$$

$$\text{I.C.: at } t = 0 \quad S_i = 0 \quad (14)$$

$$\text{B.C.1: at } r = 0 \quad S_0 = S_1 \quad (15)$$

$$\text{At } r = R \quad S_b^{n+1} = S_b^n - \frac{3m_c D_s \Delta t}{V_r R \rho_c \Delta r} (S_R^n - S_{R-1}^n) \quad (16)$$

The best fitting, shown in Figure 17-a, was obtained at  $D_s$  of  $3 \times 10^{-12}$  cm<sup>2</sup>/h. The internal diffusion-reaction of the substrate inside the ZIF-8 is described by the results shown in Table 6. It was clearly seen that the substrate concentration drops significantly within the ZIF crystal, which suggests that the reaction is more dominant than the diffusion. This result agrees with the one shown in Figure 16, which indicates that encapsulated enzyme in ZIF-8 had a lower activity than the adsorbed one, despite the higher capacity. Owing to the small size of the ZIF-8 pores, most of the reaction took place at the outer region of the ZIF-8 crystal, and the distribution of the enzyme across the pores of the ZIF-8 resulted in the lower activity. This finding, which was further confirmed by the diffusion-reaction model, limits the application of ZIF-8 for enzyme immobilization to a great extent. Synthesis of ZIF with macropores would solve this problem, and the authors of this work has recently synthesized macroporous ZIF-8 using polystyrene (PS) nanosphere as a template [19]. However, only post-synthesis adsorption was tested using the macroporous ZIF-8, and more work need to be done on the encapsulation and applying the diffusion-reaction model on it.

To verify the model prediction, an additional experiment was carried out at an initial substrate concentration of 50 mg/ml. Figure 17-b shows the comparison between the experimental data at 50 mg/ml and the model predictions, using the same diffusion coefficient determined by fitting the data at 100 mg/ml. Although, the model underestimated the drop in the substrate concentration, the overall prediction was fairly good. The significance of the model is on using experimental data to determine

diffusion and kinetics parameters and to describe the behavior of a reaction-diffusion systems within a support matrix with immobilized enzyme. More accurate values of the kinetics and diffusion parameters can be determined, and a better prediction can be obtained by fitting a larger number of experimental data at a wider range of operating conditions. Further improvement in the prediction of the diffusion-reaction model could also be achieved by using a more comprehensive kinetics model.

Table 6 : Changes in substrate concentration inside ZIF-8 crystal with time

	0.0E+00	4.5E-06	9.0E-06	1.4E-05	1.8E-05	2.3E-05	2.7E-05	3.2E-05	3.6E-05	4.1E-05
	Substrate concentration inside the ZIF crystal									
0.0	0.0E+00	0.0E+00	0.0E+00	0.0E+00	0.0E+00	0.0E+00	0.0E+00	0.0E+00	0.0E+00	0.0E+00
0.6	0.0E+00	0.0E+00	0.0E+00	0.0E+00	0.0E+00	0.0E+00	0.0E+00	0.0E+00	0.0E+00	0.0E+00
1.2	0.0E+00	0.0E+00	0.0E+00	0.0E+00	0.0E+00	0.0E+00	0.0E+00	0.0E+00	0.0E+00	0.0E+00
1.8	0.0E+00	0.0E+00	0.0E+00	0.0E+00	0.0E+00	0.0E+00	0.0E+00	0.0E+00	0.0E+00	0.0E+00
2.4	0.0E+00	0.0E+00	0.0E+00	0.0E+00	0.0E+00	0.0E+00	0.0E+00	0.0E+00	0.0E+00	0.0E+00
3.0	0.0E+00	0.0E+00	0.0E+00	0.0E+00	0.0E+00	0.0E+00	0.0E+00	0.0E+00	0.0E+00	0.0E+00
3.6	0.0E+00	0.0E+00	0.0E+00	0.0E+00	0.0E+00	0.0E+00	0.0E+00	0.0E+00	0.0E+00	0.0E+00
4.2	0.0E+00	0.0E+00	0.0E+00	0.0E+00	0.0E+00	0.0E+00	0.0E+00	0.0E+00	0.0E+00	0.0E+00
4.8	0.0E+00	0.0E+00	0.0E+00	0.0E+00	0.0E+00	0.0E+00	0.0E+00	0.0E+00	0.0E+00	0.0E+00
5.4	0.0E+00	0.0E+00	0.0E+00	0.0E+00	0.0E+00	0.0E+00	0.0E+00	0.0E+00	0.0E+00	0.0E+00
6.0	0.0E+00	0.0E+00	0.0E+00	0.0E+00	0.0E+00	0.0E+00	0.0E+00	0.0E+00	0.0E+00	2.9E-07
6.6	0.0E+00	0.0E+00	0.0E+00	0.0E+00	0.0E+00	0.0E+00	0.0E+00	0.0E+00	2.6E-08	2.9E-07
7.2	0.0E+00	0.0E+00	0.0E+00	0.0E+00	0.0E+00	0.0E+00	0.0E+00	2.3E-09	2.6E-08	3.1E-07
7.8	0.0E+00	0.0E+00	0.0E+00	0.0E+00	0.0E+00	0.0E+00	2.1E-10	2.3E-09	2.8E-08	3.0E-07
8.4	0.0E+00	0.0E+00	0.0E+00	0.0E+00	0.0E+00	1.8E-11	2.0E-10	2.5E-09	2.7E-08	3.0E-07
9.0	0.0E+00	0.0E+00	0.0E+00	0.0E+00	1.6E-12	1.8E-11	2.2E-10	2.4E-09	2.7E-08	3.0E-07
9.6	0.0E+00	0.0E+00	0.0E+00	1.4E-13	1.6E-12	2.0E-11	2.2E-10	2.4E-09	2.7E-08	2.9E-07
10.2	0.0E+00	0.0E+00	1.3E-14	1.4E-13	1.8E-12	2.0E-11	2.2E-10	2.4E-09	2.6E-08	2.9E-07
10.8	1.1E-15	1.1E-15	1.3E-14	1.6E-13	1.8E-12	1.9E-11	2.1E-10	2.4E-09	2.6E-08	2.9E-07
11.4	1.2E-15	1.2E-15	1.4E-14	1.6E-13	1.7E-12	1.9E-11	2.1E-10	2.3E-09	2.6E-08	2.8E-07
12.0	1.4E-15	1.4E-15	1.4E-14	1.6E-13	1.7E-12	1.9E-11	2.1E-10	2.3E-09	2.5E-08	2.8E-07
12.6	1.4E-15	1.4E-15	1.4E-14	1.5E-13	1.7E-12	1.9E-11	2.1E-10	2.3E-09	2.5E-08	2.8E-07
13.2	1.4E-15	1.4E-15	1.4E-14	1.5E-13	1.7E-12	1.9E-11	2.0E-10	2.3E-09	2.5E-08	2.7E-07

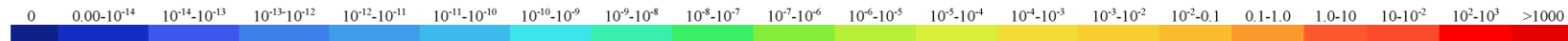




Table 6: Changes in substrate concentration inside ZIF-8 crystal with time (Continued)

	4.5E-05	5.0E-05	5.4E-05	5.9E-05	6.3E-05	6.8E-05	7.2E-05	7.7E-05	8.1E-05	8.6E-05
	Substrate concentration inside the ZIF crystal									
0.0	0.0E+00	0.0E+00	0.0E+00	0.0E+00	0.0E+00	0.0E+00	0.0E+00	0.0E+00	0.0E+00	9.5E+03
0.6	0.0E+00	0.0E+00	0.0E+00	0.0E+00	0.0E+00	0.0E+00	0.0E+00	0.0E+00	8.4E+02	9.4E+03
1.2	0.0E+00	0.0E+00	0.0E+00	0.0E+00	0.0E+00	0.0E+00	0.0E+00	7.5E+01	8.3E+02	9.3E+03
1.8	0.0E+00	0.0E+00	0.0E+00	0.0E+00	0.0E+00	0.0E+00	6.7E+00	7.4E+01	8.3E+02	9.1E+03
2.4	0.0E+00	0.0E+00	0.0E+00	0.0E+00	0.0E+00	5.9E-01	6.6E+00	7.4E+01	8.2E+02	9.0E+03
3.0	0.0E+00	0.0E+00	0.0E+00	0.0E+00	5.3E-02	5.9E-01	6.7E+00	7.3E+01	8.1E+02	8.9E+03
3.6	0.0E+00	0.0E+00	0.0E+00	4.7E-03	5.2E-02	6.0E-01	6.6E+00	7.3E+01	8.0E+02	8.8E+03
4.2	0.0E+00	0.0E+00	4.2E-04	4.6E-03	5.3E-02	5.9E-01	6.5E+00	7.2E+01	7.9E+02	8.7E+03
4.8	0.0E+00	3.7E-05	4.1E-04	4.8E-03	5.3E-02	5.8E-01	6.4E+00	7.1E+01	7.8E+02	8.6E+03
5.4	3.3E-06	3.7E-05	4.3E-04	4.7E-03	5.2E-02	5.8E-01	6.3E+00	7.0E+01	7.7E+02	8.5E+03
6.0	3.2E-06	3.8E-05	4.2E-04	4.7E-03	5.2E-02	5.7E-01	6.3E+00	6.9E+01	7.6E+02	8.4E+03
6.6	3.4E-06	3.8E-05	4.2E-04	4.6E-03	5.1E-02	5.6E-01	6.2E+00	6.8E+01	7.5E+02	8.3E+03
7.2	3.4E-06	3.8E-05	4.1E-04	4.6E-03	5.0E-02	5.6E-01	6.1E+00	6.7E+01	7.4E+02	8.2E+03
7.8	3.4E-06	3.7E-05	4.1E-04	4.5E-03	5.0E-02	5.5E-01	6.0E+00	6.7E+01	7.3E+02	8.1E+03
8.4	3.3E-06	3.7E-05	4.0E-04	4.5E-03	4.9E-02	5.4E-01	6.0E+00	6.6E+01	7.3E+02	8.0E+03
9.0	3.3E-06	3.6E-05	4.0E-04	4.4E-03	4.9E-02	5.4E-01	5.9E+00	6.5E+01	7.2E+02	7.9E+03
9.6	3.2E-06	3.6E-05	3.9E-04	4.4E-03	4.8E-02	5.3E-01	5.8E+00	6.4E+01	7.1E+02	7.8E+03
10.2	3.2E-06	3.5E-05	3.9E-04	4.3E-03	4.7E-02	5.2E-01	5.8E+00	6.3E+01	7.0E+02	7.7E+03
10.8	3.2E-06	3.5E-05	3.9E-04	4.2E-03	4.7E-02	5.2E-01	5.7E+00	6.3E+01	6.9E+02	7.6E+03
11.4	3.1E-06	3.5E-05	3.8E-04	4.2E-03	4.6E-02	5.1E-01	5.6E+00	6.2E+01	6.8E+02	7.5E+03
12.0	3.1E-06	3.4E-05	3.8E-04	4.1E-03	4.6E-02	5.0E-01	5.6E+00	6.1E+01	6.7E+02	7.4E+03
12.6	3.1E-06	3.4E-05	3.7E-04	4.1E-03	4.5E-02	5.0E-01	5.5E+00	6.0E+01	6.7E+02	7.3E+03
13.2	3.0E-06	3.3E-05	3.7E-04	4.0E-03	4.5E-02	4.9E-01	5.4E+00	6.0E+01	6.6E+02	7.3E+03

Table 6: Changes in substrate concentration inside ZIF-8 crystal with time (Continued)

	0.0E+00	4.5E-06	9.0E-06	1.4E-05	1.8E-05	2.3E-05	2.7E-05	3.2E-05	3.6E-05	4.1E-05
	Substrate concentration inside the ZIF crystal									
13.8	1.4E-15	1.4E-15	1.4E-14	1.5E-13	1.7E-12	1.8E-11	2.0E-10	2.2E-09	2.5E-08	2.7E-07
14.4	1.3E-15	1.3E-15	1.4E-14	1.5E-13	1.6E-12	1.8E-11	2.0E-10	2.2E-09	2.4E-08	2.7E-07
15.0	1.3E-15	1.3E-15	1.3E-14	1.5E-13	1.6E-12	1.8E-11	2.0E-10	2.2E-09	2.4E-08	2.6E-07
15.6	1.3E-15	1.3E-15	1.3E-14	1.5E-13	1.6E-12	1.8E-11	1.9E-10	2.1E-09	2.4E-08	2.6E-07
16.2	1.3E-15	1.3E-15	1.3E-14	1.4E-13	1.6E-12	1.7E-11	1.9E-10	2.1E-09	2.3E-08	2.6E-07
16.8	1.3E-15	1.3E-15	1.3E-14	1.4E-13	1.6E-12	1.7E-11	1.9E-10	2.1E-09	2.3E-08	2.5E-07
17.4	1.3E-15	1.3E-15	1.3E-14	1.4E-13	1.5E-12	1.7E-11	1.9E-10	2.1E-09	2.3E-08	2.5E-07
18.0	1.2E-15	1.2E-15	1.3E-14	1.4E-13	1.5E-12	1.7E-11	1.9E-10	2.0E-09	2.3E-08	2.5E-07
18.6	1.2E-15	1.2E-15	1.2E-14	1.4E-13	1.5E-12	1.7E-11	1.8E-10	2.0E-09	2.2E-08	2.5E-07
19.2	1.2E-15	1.2E-15	1.2E-14	1.4E-13	1.5E-12	1.6E-11	1.8E-10	2.0E-09	2.2E-08	2.4E-07
19.8	1.2E-15	1.2E-15	1.2E-14	1.3E-13	1.5E-12	1.6E-11	1.8E-10	2.0E-09	2.2E-08	2.4E-07
20.4	1.2E-15	1.2E-15	1.2E-14	1.3E-13	1.5E-12	1.6E-11	1.8E-10	1.9E-09	2.1E-08	2.4E-07
21.0	1.2E-15	1.2E-15	1.2E-14	1.3E-13	1.4E-12	1.6E-11	1.7E-10	1.9E-09	2.1E-08	2.3E-07
21.6	1.2E-15	1.2E-15	1.2E-14	1.3E-13	1.4E-12	1.6E-11	1.7E-10	1.9E-09	2.1E-08	2.3E-07
22.2	1.1E-15	1.1E-15	1.2E-14	1.3E-13	1.4E-12	1.5E-11	1.7E-10	1.9E-09	2.1E-08	2.3E-07
22.8	1.1E-15	1.1E-15	1.1E-14	1.3E-13	1.4E-12	1.5E-11	1.7E-10	1.9E-09	2.0E-08	2.3E-07
23.4	1.1E-15	1.1E-15	1.1E-14	1.2E-13	1.4E-12	1.5E-11	1.7E-10	1.8E-09	2.0E-08	2.2E-07
24.0	1.1E-15	1.1E-15	1.1E-14	1.2E-13	1.4E-12	1.5E-11	1.6E-10	1.8E-09	2.0E-08	2.2E-07

Table 6: Changes in substrate concentration inside ZIF-8 crystal with time (Continued)

	4.5E-05	5.0E-05	5.4E-05	5.9E-05	6.3E-05	6.8E-05	7.2E-05	7.7E-05	8.1E-05	8.6E-05									
	Substrate concentration inside the ZIF crystal																		
13.8	3.0E-06	3.3E-05	3.6E-04	4.0E-03	4.4E-02	4.9E-01	5.4E+00	5.9E+01	6.5E+02	7.2E+03									
14.4	2.9E-06	3.2E-05	3.6E-04	3.9E-03	4.4E-02	4.8E-01	5.3E+00	5.8E+01	6.4E+02	7.1E+03									
15.0	2.9E-06	3.2E-05	3.5E-04	3.9E-03	4.3E-02	4.7E-01	5.2E+00	5.8E+01	6.3E+02	7.0E+03									
15.6	2.9E-06	3.2E-05	3.5E-04	3.9E-03	4.2E-02	4.7E-01	5.2E+00	5.7E+01	6.3E+02	6.9E+03									
16.2	2.8E-06	3.1E-05	3.5E-04	3.8E-03	4.2E-02	4.6E-01	5.1E+00	5.6E+01	6.2E+02	6.8E+03									
16.8	2.8E-06	3.1E-05	3.4E-04	3.8E-03	4.1E-02	4.6E-01	5.0E+00	5.5E+01	6.1E+02	6.7E+03									
17.4	2.8E-06	3.1E-05	3.4E-04	3.7E-03	4.1E-02	4.5E-01	5.0E+00	5.5E+01	6.0E+02	6.7E+03									
18.0	2.7E-06	3.0E-05	3.3E-04	3.7E-03	4.0E-02	4.5E-01	4.9E+00	5.4E+01	6.0E+02	6.6E+03									
18.6	2.7E-06	3.0E-05	3.3E-04	3.6E-03	4.0E-02	4.4E-01	4.9E+00	5.4E+01	5.9E+02	6.5E+03									
19.2	2.7E-06	2.9E-05	3.2E-04	3.6E-03	3.9E-02	4.3E-01	4.8E+00	5.3E+01	5.8E+02	6.4E+03									
19.8	2.6E-06	2.9E-05	3.2E-04	3.5E-03	3.9E-02	4.3E-01	4.7E+00	5.2E+01	5.8E+02	6.3E+03									
20.4	2.6E-06	2.9E-05	3.2E-04	3.5E-03	3.9E-02	4.2E-01	4.7E+00	5.2E+01	5.7E+02	6.3E+03									
21.0	2.6E-06	2.8E-05	3.1E-04	3.5E-03	3.8E-02	4.2E-01	4.6E+00	5.1E+01	5.6E+02	6.2E+03									
21.6	2.5E-06	2.8E-05	3.1E-04	3.4E-03	3.8E-02	4.1E-01	4.6E+00	5.0E+01	5.5E+02	6.1E+03									
22.2	2.5E-06	2.8E-05	3.1E-04	3.4E-03	3.7E-02	4.1E-01	4.5E+00	5.0E+01	5.5E+02	6.0E+03									
22.8	2.5E-06	2.7E-05	3.0E-04	3.3E-03	3.7E-02	4.0E-01	4.5E+00	4.9E+01	5.4E+02	6.0E+03									
23.4	2.5E-06	2.7E-05	3.0E-04	3.3E-03	3.6E-02	4.0E-01	4.4E+00	4.9E+01	5.3E+02	5.9E+03									
0	0.00-10 <sup>-14</sup>	10 <sup>-14</sup> -10 <sup>-13</sup>	10 <sup>-13</sup> -10 <sup>-12</sup>	10 <sup>-12</sup> -10 <sup>-11</sup>	10 <sup>-11</sup> -10 <sup>-10</sup>	10 <sup>-10</sup> -10 <sup>-9</sup>	10 <sup>-9</sup> -10 <sup>-8</sup>	10 <sup>-8</sup> -10 <sup>-7</sup>	10 <sup>-7</sup> -10 <sup>-6</sup>	10 <sup>-6</sup> -10 <sup>-5</sup>	10 <sup>-5</sup> -10 <sup>-4</sup>	10 <sup>-4</sup> -10 <sup>-3</sup>	10 <sup>-3</sup> -10 <sup>-2</sup>	10 <sup>-2</sup> -0.1	0.1-1.0	1.0-10	10-10 <sup>2</sup>	10 <sup>2</sup> -10 <sup>3</sup>	>1000

## Chapter 4: Conclusion

This thesis was focusing on encapsulated lipase into the ZIF-8. Under moderate conditions, lipase was successfully encapsulated into hexagonal ZIF-8 crystals to be used in biodiesel production. The encapsulation did not affect the ZIF-8 crystals and resulted in a more stable immobilized lipase. A diffusion-reaction model was developed and solved numerically to provide a better understanding of how the reaction occurs inside the ZIF-8 crystal. The diffusion-reaction model used in this work is the first one to be reported in literature, which gives an insight into how the reaction takes place inside ZIF-8 encapsulated with lipase. The model can be applied to any diffusion-reaction systems and can be further improved to consider more accurate surface reaction models. In summary, the results of this work hold potential to significantly simplify the production of biodiesel from the L-ZIF.

## References

- Adnan, M., Li, K., Wang, J., Xu, L., & Yan, Y. (2018). Hierarchical ZIF-8 Toward Immobilizing Burkholderia Cepacia Lipase for Application in Biodiesel Preparation [online]. *International Journal of Molecular Sciences*, 19(5), 1424-1438. (Accessed 24/8/2019). Retrieved from: <https://doi.org/10.3390/ijms19051424>
- Adnan, M., Li, K., Xu, L., & Yan, Y. (2018). X-Shaped ZIF-8 for Immobilization Rhizomucor Miehei Lipase via Encapsulation and Its Application Toward Biodiesel Production [online]. *Catalysts*, 8, 96-110. (Accessed 28/6/2020). Retrieved from: <https://doi.org/10.3390/catal8030096>.
- Antizar-Ladislao, B., & Turrion-Gomes, J. (2008). Second-Generation Biofuels and Local Bioenergy Systems [online]. *Biofuels, Bioproducts and Biorefining*, 2(5), 455-69. (Accessed 14/05/2020). Retrieved from: <https://doi.org/10.1002/bbb.97>.
- Asunción Molina, M., Gascón-Pérez, V., Sánchez-Sánchez, M., & Blanco, R. M. (2021). Sustainable One-Pot Immobilization of Enzymes in/on Metal-Organic Framework Materials [online]. *Catalysts*, 2(5), 455-469. (Accessed 14/5/2020). Retrieved from: <https://doi.org/10.1002/bbb.97>.
- Batool, F., Akbar, J., Iqbal, S., Noreen, S., & Bukhari, S. N. A. (2018). Study of Isothermal, Kinetic, and Thermodynamic Parameters for Adsorption of Cadmium: An Overview of Linear and Nonlinear Approach and Error Analysis [online]. *Bioinorganic Chemistry and Applications*, 2018, 1-11. (Accessed 20/5/2021). Retrieved from: <https://doi.org/10.1155/2018/3463724>.
- Begum, J., Hussain, Z., & Noor, T. (2020). Adsorption and kinetic study of Cr(VI) on ZIF-8 based composites [online]. *Materials Research Express*, 7(1), 1-13. (Accessed 2/4/2021). Retrieved from: <https://doi.org/10.1088/2053-1591/ab6b66>.
- Boon-anuwat, N., Kiatkittipong, W., Aiouache, F., & Assabumrungrat, S. (2015). Process Design of Continuous Biodiesel Production by Reactive Distillation: Comparison Between Homogeneous and Heterogeneous Catalysts [online]. *Chemical Engineering and Processing: Process Intensification*, 92, 33-44. (Accessed 29/5/2020). Retrieved from: <https://doi.org/10.1016/j.cep.2015.03.025>.

- Boundy, J. A., Smiley, K. L., Swanson, C. L., & Hofreiter, B. T. (1976). Exoenzymic Activity of Alpha-Amylase Immobilized on A Phenol-Formaldehyde Resin [online]. *Carbohydrate Research*, 48(2), 239-244. (Accessed 21/5/2021). Retrieved from: [https://doi.org/10.1016/S0008-6215\(00\)83219-X](https://doi.org/10.1016/S0008-6215(00)83219-X).
- Branco, R., Serafim, L., & Xavier, A. (2018). Second Generation Bioethanol Production: on the Use of Pulp and Paper Industry Wastes as Feedstock [online]. *Fermentation*, 5, 4-34. (Accessed 16/5/2020). Retrieved from: <https://doi.org/10.3390/fermentation5010004>.
- Brena, B., González-Pombo, P., & Batista-Viera, F. (2013). Immobilization of Enzymes: A Literature Survey [online]. *Methods in Molecular Biology (Clifton, N.J.)*, 1051, 15-31. (Accessed 21/5/2021). Retrieved from: [https://doi.org/10.1007/978-1-62703-550-7\\_2](https://doi.org/10.1007/978-1-62703-550-7_2)
- Çakmakçi, E., Muhsir, P., & Demir, S. (2017). Physical and Covalent Immobilization of Lipase onto Amine Groups Bearing Thiol-Ene Photocured Coatings [online]. *Applied Biochemistry and Biotechnology*, 181(3), 1030-1047. (Accessed 20/5/2021). Retrieved from: <https://doi.org/10.1007/s12010-016-2266-6>.
- Cao, Y., Wu, Z., Wang, T., Xiao, Y., Huo, Q., & Liu, Y. (2016). Immobilization of Bacillus Subtilis Lipase on a Cu-BTC Based Hierarchically Porous Metal–Organic Framework Material: A Biocatalyst for Esterification [online]. *Dalton Transactions*, 45(16), 6998-7003. (Accessed 2/3/2021). Retrieved from: <https://doi.org/10.1039/C6DT00677A>.
- Cardenas, F., Alvarez, E., Castro-Alvarez, M.-S., Montero, Jose Maria, Valmaseda, M., Elson, S., & Sinisterra, J.-V. (2001). Screening and Catalytic Activity in Organic Synthesis of Novel Fungal and Yeast Lipases [online]. *Journal of Molecular Catalysis B: Enzymatic*, 14, 111-123. (Accessed 20/5/2021). Retrieved from: [https://doi.org/10.1016/S1381-1177\(00\)00244-7](https://doi.org/10.1016/S1381-1177(00)00244-7).
- Chen, L., Zhang, X., Cheng, X., Xie, Z., Kuang, Q., & Zheng, L. (2020). The Function of Metal–Organic Frameworks in the Application of MOF-Based Composites [online]. *Nanoscale Advances*, 2(7), 2628-2647. (Accessed 21/5/2021). Retrieved from: <https://doi.org/10.1039/D0NA00184H>.
- Corma, A., García, H., & Llabrés i Xamena, F. X. (2010). Engineering Metal Organic Frameworks for Heterogeneous Catalysis [online]. *Chemical Reviews*, 110(8), 4606-4655. (Accessed 13/3/2021). Retrieved from: <https://doi.org/10.1021/cr9003924>.

- Czaja, A. U., Trukhan, N., & Müller, U. (2009). Industrial Applications of Metal–Organic Frameworks. *Chemical Society Reviews*, 38(5), 1284-1293. (Accessed 13/3/2021). Retrieved from: <https://doi.org/10.1039/B804680H>.
- Datta, A., Hossain, A., & Roy, S. (2019). An Overview on Biofuels and Their Advantages and Disadvantages [online]. *Asian Journal of Chemistry*, 31(8), 1851-1858. (Accessed 17/5/2020). Retrieved from: <https://doi.org/10.14233/ajchem.2019.22098>
- Dias Gomes, M., & Woodley, J. (2019). Considerations When Measuring Biocatalyst Performance [online]. *Molecules*, 24(19), 3573-3584. (Accessed 20/5/2021). Retrieved from: <https://doi.org/10.3390/molecules24193573>.
- Du, Y., Gao, J., Zhou, L., Ma, L., He, Y., Huang, Z., & Jiang, Y. (2017). Enzyme Nanocapsules Armored by Metal–Organic Frameworks: A Novel Approach for Preparing Nanobiocatalyst [online]. *Chemical Engineering Journal*, 327, 1192-1197. (Accessed 13/8/2020). Retrieved from: <https://doi.org/10.1016/j.cej.2017.07.021>
- Engel, E. R., & Scott, J. L. (2020). Advances in the Green Chemistry of Coordination Polymer Materials [online]. *Green Chemistry*, 22(12), 3693-3715. (Accessed 20/5/2021). Retrieved from: <https://doi.org/10.1039/D0GC01074J>
- Ferreira, R., Menezes, R., Sampaio, K., & Batista, E. (2020). Heterogeneous Catalysts for Biodiesel Production: A Review [online]. *Food and Public Health*, 9(4), 125-137. (Accessed 22/11/2021). Retrieved from: <https://doi.org/10.5923/j.fph.20190904.04>
- Filho, D. G., Silva, A. G., & Guidini, C. Z. (2019). Lipases: Sources, Immobilization Methods, and Industrial Applications [online]. *Applied Microbiology and Biotechnology*, 103(18), 7399-7423. (Accessed 1/6/2020). Retrieved from: <https://doi.org/10.1007/s00253-019-10027-6>
- Garmroodi, M., Mohammadi, M., Ramazani, A., Ashjari, M., Mohammadi, J., Sabour, B., & Yousefi, M. (2016). Covalent Binding of Hyper-Activated Rhizomucor Miehei Lipase (RML) on Hetero-Functionalized Siliceous Supports [online]. *International Journal of Biological Macromolecules*, 86, 208-215. (Accessed 8/5/2021). Retrieved from: <https://doi.org/10.1016/j.ijbiomac.2016.01.076>
- Ge, J., Yang, C., Zhu, J., Lu, D., & Liu, Z. (2012). Nanobiocatalysis in Organic Media: Opportunities for Enzymes in Nanostructures [online]. *Topics in*

*Catalysis*, 55(16), 1070-1080. (Accessed 19/5/2021). Retrieved from: <https://doi.org/10.1007/s11244-012-9906-z>

Ghadiryafar, M., Rosentrater, K. A., Keyhani, A., & Omid, M. (2016). A Review of Macroalgae Production, with Potential Applications in Biofuels and Bioenergy [online]. *Renewable and Sustainable Energy Reviews*, 54, 473-481. (Accessed 6/2/2018). Retrieved from: <https://doi.org/10.1016/j.rser.2015.10.022>

Guzik, U., Hupert-Kocurek, K., & Wojcieszynska, D. (2014). Immobilization as a Strategy for Improving Enzyme Properties-Application to Oxidoreductases [online]. *Molecules (Basel, Switzerland)*, 19(7), 8995-9018. (Accessed 14/10/2021). Retrieved from: <https://doi.org/10.3390/molecules19078995>

Homaei, A. A., Sariri, R., Vianello, F., & Stevanato, R. (2013). Enzyme Immobilization: An Update [online]. *Journal of Chemical Biology*, 6(4), 185-205. (Accessed 20/5/2021). Retrieved from: <https://doi.org/10.1007/s12154-013-0102-9>

Hosseini, S. E., & Wahid, M. A. (2015). Utilization of Biogas Released from Palm Oil Mill Effluent for Power Generation Using Self-Preheated Reactor [online]. *Energy Conversion and Management*, 105, 957-966. (Accessed 11/9/2019). Retrieved from: <https://doi.org/10.1016/j.enconman.2015.08.058>.

Hu, Y., Dai, L., Liu, D., & Du, W. (2020). Hydrophobic Pore Space Constituted in Macroporous ZIF-8 for Lipase Immobilization Greatly Improving Lipase Catalytic Performance in Biodiesel Preparation [online]. *Biotechnology for Biofuels*, 13(1), 86-95. (Accessed 2/3/2021). Retrieved from: <https://doi.org/10.1186/s13068-020-01724-w>

Ismail, M., & Al-Zuhair, S. (2020). Thermo-Responsive Switchable Solvents for Simultaneous Microalgae Cell Disruption, Oil Extraction-Reaction, and Product Separation for Biodiesel Production [online]. *Biocatalysis and Agricultural Biotechnology*, 26, 1-9, (Accessed 25/9/2021). Retrieved from: <https://doi.org/10.1016/j.bcab.2020.101667>

Jesionowski, T., Zdarta, J., & Krajewska, B. (2014). Enzyme Immobilization by Adsorption: A Review [online]. *Adsorption*, 20(5-6), 801-821. (Accessed 16/10/2021). Retrieved from: <https://doi.org/10.1007/s10450-014-9623-y>

Ke, C., Li, X., Huang, S., Xu, L., & Yan, Y. (2014). Enhancing Enzyme Activity and Enantioselectivity of Burkholderia Cepacia Lipase Via Immobilization on Modified Multi-Walled Carbon Nanotubes [online]. *RSC Advances*, 4(101),



57810-57818. (Accessed 8/5/2021). Retrieved from:  
<https://doi.org/10.1039/C4RA10517F>.

Klibanov, A. M. (2001). Improving Enzymes by Using Them in Organic Solvents [online]. *Nature*, 409(6817), 241-246. (Accessed 26/9/2021). Retrieved from:  
<https://doi.org/10.1038/35051719>

Koh, K., Wong-Foy, A. G., & Matzger, A. J. (2009). MOF@MOF: Microporous Core–Shell Architectures [online]. *Chemical Communications*, (41), 6162-6164. (Accessed 13/3/2021). Retrieved from:  
<https://doi.org/10.1039/B904526K>

Kumar, A., Dhar, K., Kanwar, S. S., & Arora, P. K. (2016). Lipase Catalysis in Organic Solvents: Advantages and Applications [online]. *Biological Procedures Online*, 18(1), 2-13. (Accessed 18/5/2021). Retrieved from:  
<https://doi.org/10.1186/s12575-016-0033-2>

Liu, H. F., Ma, J., Winter, C., & Bayer, R. (2010). Recovery and Purification Process Development for Monoclonal Antibody Production [online]. *MAbs*, 2(5), 480-499. (Accessed 20/5/2021). Retrieved from:  
<https://doi.org/10.4161/mabs.2.5.12645>

Liu, N.-L., Dutta, S., Salunkhe, R. R., Ahamad, T., Alshehri, S. M., Yamauchi, Y., ... Wu, K. C.-W. (2016). ZIF-8 Derived, Nitrogen-Doped Porous Electrodes of Carbon Polyhedron Particles for High-Performance Electrosorption of Salt Ions [online]. *Scientific Reports*, 6(1), 28847-28854. (Accessed 2/4/2021). Retrieved from: <https://doi.org/10.1038/srep28847>

Liu, Y., Liu, T., Wang, X., Xu, L., & Yan, Y. (2011). Biodiesel Synthesis Catalyzed by Burkholderia Cenocepacia Lipase Supported on Macroporous Resin NKA in Solvent-Free and Isooctane Systems [online]. *Energy & Fuels*, 25(3), 1206-1212. (Accessed 23/8/2019). Retrieved from:  
<https://doi.org/10.1021/ef200066x>

Marchetti, J. M., Miguel, V. U., & Errazu, A. F. (2007). Possible Methods for Biodiesel Production [online]. *Renewable and Sustainable Energy Reviews*, 11(6), 1300-1311. (Accessed 28/10/2018). Retrieved from:  
<https://doi.org/10.1016/j.rser.2005.08.006>

Mata, T. M., Martins, A. A., & Caetano, Nidia. S. (2010). Microalgae for Biodiesel Production and Other Applications: A Review [online]. *Renewable and Sustainable Energy Reviews*, 14(1), 217-232. (Accessed 17/5/2020). Retrieved from: <https://doi.org/10.1016/j.rser.2009.07.020>

- Mello Bueno, P. R., de Oliveira, T. F., Castiglioni, G. L., Soares Júnior, M. S., & Ulhoa, C. J. (2015). Application of Lipase from *Burkholderia Cepacia* in the Degradation of Agro-Industrial Effluent [online]. *Water Science and Technology: A Journal of the International Association on Water Pollution Research*, 71(7), 957-964. (Accessed 1/6/2020). Retrieved from: <https://doi.org/10.2166/wst.2015.037>
- Misson, M., Zhang, H., & Jin, B. (2015). Nanobiocatalyst Advancements and Bioprocessing Applications [online]. *Journal of the Royal Society Interface*, 12(102), 1-20. (Accessed 19/5/2021). Retrieved from: <https://doi.org/10.1098/rsif.2014.0891>
- Mohamad, N. R., Marzuki, N. H. C., Buang, N. A., Huyop, F., & Wahab, R. A. (2015). An Overview of Technologies for Immobilization of Enzymes and Surface Analysis Techniques for Immobilized Enzymes [online]. *Biotechnology, Biotechnological Equipment*, 29(2), 205-220. (Accessed 20/5/2021). Retrieved from: <https://doi.org/10.1080/13102818.2015.1008192>
- Mokhtar, N., Rahman, R., Noor, N., Mohd Shariff, F., & Mohamad Ali, M. S. (2020). The Immobilization of Lipases on Porous Support by Adsorption and Hydrophobic Interaction Method [online]. *Catalysts*, 10, 744-761. (Accessed 20/5/2021). Retrieved from: <https://doi.org/10.3390/catal10070744>
- Moreira, K. S., Moura Júnior, L. S., Monteiro, R. R. C., de Oliveira, A. L. B., Valle, C. P., Freire, T. M., ... dos Santos, J. C. S. (2020). Optimization of the Production of Enzymatic Biodiesel from Residual Babassu Oil (*Orbignya sp.*) via RSM [online]. *Catalysts*, 10(4), 414-434. (Accessed 17/5/2021). Retrieved from: <https://doi.org/10.3390/catal10040414>
- Mu, R., Wang, Z., Wamsley, M. C., Duke, C. N., Lii, P. H., Epley, S. E., Roberts, P. J. (2020). Application of Enzymes in Regioselective and Stereoselective Organic Reactions [online]. *Catalysts*, 10(8), 832-857. (Accessed 19/5/2021). Retrieved from: <https://doi.org/10.3390/catal10080832>
- Nadar, S. S., & Rathod, V. K. (2018). Encapsulation of Lipase within Metal-Organic Framework (MOF) with Enhanced Activity Intensified Under Ultrasound [online]. *Enzyme and Microbial Technology*, 108, 11-20. (Accessed 24/6/2019). Retrieved from: <https://doi.org/10.1016/j.enzmictec.2017.08.008>
- Nelson, L. A., Foglia, T. A., & Marmer, W. N. (1996). Lipase-Catalyzed Production of Biodiesel [online]. *Journal of the American Oil Chemists' Society*, 73(9), 1191-1195. (Accessed 26/9/2021). Retrieved from: <https://doi.org/10.1007/BF02523383>

- Nguyen, H. H., & Kim, M. (2017). An Overview of Techniques in Enzyme Immobilization [online]. *Applied Science and Convergence Technology*, 26, 157-163. (Accessed 20/5/2021). Retrieved from: <https://doi.org/10.5757/ASCT.2017.26.6.157>
- Pitzalis, F., Carucci, C., Naseri, M., Fotouhi, L., Magner, E., & Salis, A. (2018). Lipase Encapsulation onto ZIF-8: A Comparison between Biocatalysts Obtained at Low and High Zinc/2-Methylimidazole Molar Ratio in Aqueous Medium [online]. *ChemCatChem*, 10(7), 1578-1585. (Accessed 23/5/2021). Retrieved from: <https://doi.org/10.1002/cctc.201701984>
- Pizarro, A. V. L., & Park, E. Y. (2003). Lipase-Catalyzed Production of Biodiesel Fuel from Vegetable Oils Contained in Waste Activated Bleaching Earth [online]. *Process Biochemistry*, 38(7), 1077-1082. (Accessed 12/3/2021). Retrieved from: <https://www.cabdirect.org/cabdirect/abstract/20043054069>.
- Rafiei, S., Tangestaninejad, S., Horcajada, P., Moghadam, M., Mirkhani, V., Mohammadpoor-Baltork, I., ... Zadehahmadi, F. (2018). Efficient Biodiesel Production Using a Lipase@ZIF-67 Nanobioreactor [online]. *Chemical Engineering Journal*, 334, 1233-1241. (Accessed 5/4/2021). Retrieved from: <https://doi.org/10.17113/ftb.56.01.18.5491>
- Raveendran, S., Parameswaran, B., Ummalyma, S. B., Abraham, A., Mathew, A. K., Madhavan, A., ... Pandey, A. (2018). Applications of Microbial Enzymes in Food Industry [online]. *Food Technology and Biotechnology*, 56(1), 16-30. (Accessed 19/5/2021). Retrieved from: <https://doi.org/10.17113/ftb.56.01.18.5491>
- Reis, C. L. B., Sousa, E. Y. A. de, Serpa, J. de F., Oliveira, R. C., Santos, J. C. S. dos, Reis, C. L. B., ... Santos, J. C. S. dos. (2019). Design of Immobilized Enzyme Biocatalysts: Drawbacks and Opportunities [online]. *Química Nova*, 42(7), 768-783. (Accessed 20/5/2021). Retrieved from: <https://doi.org/10.21577/0100-4042.20170381>
- Reis, P., Holmberg, K., Watzke, H., Leser, M. E., & Miller, R. (2009). Lipases at Interfaces: A Review [online]. *Advances in Colloid and Interface Science*, 147-148, 237-250. (Accessed 10/10/2018). Retrieved from: <https://doi.org/10.1016/j.cis.2008.06.001>
- Robinson, P. K. (2015). Enzymes: Principles and Biotechnological Applications [online]. *Essays in Biochemistry*, 59, 1-41. (Accessed 19/5/2021). Retrieved from: <https://doi.org/10.1042/bse0590001>

- Rueda, N., Santos, J. C. S. dos, Torres, R., Barbosa, O., Ortiz, C., & Fernandez-Lafuente, R. (2015). Reactivation of Lipases by the Unfolding and Refolding of Covalently Immobilized Biocatalysts [online]. *RSC Advances*, 5(68), 55588-55594. (Accessed 20/5/2021). Retrieved from: <https://doi.org/10.1039/C5RA07379K>
- Sharma, R., Chisti, Y., & Banerjee, U. C. (2001). Production, Purification, Characterization, and Applications of Lipases [online]. *Biotechnology Advances*, 19(8), 627-662. (Accessed 20/5/2021). Retrieved from: [https://doi.org/10.1016/S0734-9750\(01\)00086-6](https://doi.org/10.1016/S0734-9750(01)00086-6)
- Song, Q., Nataraj, S. K., Roussanova, M. V., Tan, J. C., Hughes, D. J., Li, W., ... Sivaniah, E. (2012). Zeolitic Imidazolate Framework (ZIF-8) based Polymer Nanocomposite Membranes for Gas Separation [online]. *Energy & Environmental Science*, 5(8), 8359-8370. (Accessed 2/3/2021). Retrieved from: <https://doi.org/10.1039/c2ee21996d>
- Su, E., & Wei, D. (2008). Improvement in Lipase-Catalyzed Methanolysis of Triacylglycerols for Biodiesel Production Using a Solvent Engineering Method [online]. *Journal of Molecular Catalysis B: Enzymatic*, 55(3-4), 118-125. (Accessed 25/9/2021). Retrieved from: <https://doi.org/10.1016/j.molcatb.2008.03.001>
- Sulaiman, A.-Z. (2007). Production of Biodiesel: Possibilities and Challenges [online]. *Biofuels, Bioproducts and Biorefining*, 1, 57-66. (Accessed 27/9/2021). Retrieved from: <https://doi.org/10.1002/bbb.2>
- Tan, T., Nie, K., & Wang, F. (2006). Production of Biodiesel by Immobilized *Candida* sp. Lipase at High Water Content [online]. *Applied Biochemistry and Biotechnology*, 128, 109-116. (Accessed 19/5/2021). Retrieved from: <http://dx.doi.org.uaeu.idm.oclc.org/10.1385/ABAB:128:2:109>
- Vieille, C., & Zeikus, G. J. (2001). Hyperthermophilic Enzymes: Sources, Uses, and Molecular Mechanisms for Thermostability [online]. *Microbiology and Molecular Biology Reviews*, 65(1), 1-43. (Accessed 20/5/2021). Retrieved from: <https://doi.org/10.1128/MMBR.65.1.1-43.2001>
- Wahab, R. A., Elias, N., Abdullah, F., & Ghoshal, S. K. (2020). On the Taught New Tricks of Enzymes Immobilization: An All-Inclusive Overview [online]. *Reactive and Functional Polymers*, 152, 104613-104639. (Accessed 20/5/2021). Retrieved from: <https://doi.org/10.1016/j.reactfunctpolym.2020.104613>

West, Alex H., Dusko Posarac, and Naoko Ellis (2008). Assessment of Four Biodiesel Production Processes Using HYSYS Plant [online]. *Bioresource Technology* 99(14), 6587-6601. (Accessed 29/5/2020). Retrieved from: <https://doi.org/10.1016/j.biortech.2007.11.046>.

Winkler, C. K., Schrittwieser, J. H., & Kroutil, W. (2021). Power of Biocatalysis for Organic Synthesis [online]. *ACS Central Science*, 7(1), 55–71. (Accessed 19/5/2021). Retrieved from: <https://doi.org/10.1021/acscentsci.0c01496>

## List of Publications

- Al-Mansouri, R., Du, W., Al-Zuhair, S., 2021. Reaction-diffusion model to describe biodiesel production using lipase encapsulated in ZIF-8. Fuel 122630. <https://doi.org/10.1016/j.fuel.2021.122630>

## Appendix



Figure A-1: Gas chromatography (GC) (Shimadzu, GC-2010, Japan)



Figure A-2: Gas physisorption instrument (TriStar II 3020 Analyzer, Japan)





Figure A-3: Fourier transform infrared (FT-IR) (JASCO FT/IR-4700, Japan)